Design and Development of Loitering Munition UAV

By

M. Ayaz Mahmood

319116

Supervisor

Dr. Adnan Maqsood

School of Interdisciplinary Engineering and Sciences

National University of Sciences and Technology

Islamabad, Pakistan

August 2023

Design and Development of Loitering Munition UAV

By

M. Ayaz Mahmood

319116

A thesis submitted in partial fulfillment of the requirements for the degree of

MS Systems Engineering

Thesis Supervisor:

Dr. Adnan Maqsood

School of Interdisciplinary Engineering and Sciences

National University of Sciences and Technology,

Islamabad, Pakistan

August 2023

Annex A to NUST Letter No. 0972/102/Exams/Thesis-Cert dated 23 Dec 16.

THESIS ACCEPTANCE CERTIFICATE

Certified that final copy of MS/MPhil thesis written by Mr M. AYAZ MAHMOOD Registration No. 319118 of SINES has been vetted by undersigned, found complete in all aspects as per NUST Statutes/Regulations, is free of plagiarism, errors, and mistakes and is accepted as partial fulfillment for award of MS degree. It is further certified that necessary amendments as pointed out by GEC members of the scholar have also been incorporated in the said thesis.

Signature with stamp: [signature]

Name of Supervisor: ADNAN MAQSOOD

Date: 25 Aug 23

Signature of HoD with stamp: [signature]

Dr. Mian Ilyas Ahmad
HoD Engineering
Professor
SINES - NUST, Sector H-12
Islamabad

Date: 25 Aug 2023

Countersign by

Signature (Dean/Principal): [signature]

Date: 28/08/2023.

Declaration

I certify that this research work titled "*Design and Development of Loitiring Munition UAV"* is my own work. The work has not been presented elsewhere for assessment.

I confirm that:

1. This work was done wholly or mainly while in candidature for a Master of Science degree at NUST.

2. Where any part of this thesis has been previously submitted for a degree or any other qualification at NUST or any other institution, this has been clearly stated.

3. Where I have consulted the published work of others, this is always clearly attributed.

4. Where I have quoted from the work of others, the source is always given. With the exception of such quotations, this thesis is entirely my own work.

5. I have acknowledged all main sources of help.

6. Where the thesis is based on worked done by myself jointly with others, I have made clear exactly what was done by others, and I have contributed myself.

M. Ayaz Mahmood

2019-NUST-MS-SE-319116

Acknowledgments

I would like to begin by expressing my deepest gratitude to Allah, whose guidance and blessings have been instrumental in my ability to complete this thesis. I am eternally grateful for the support and love my parents have provided me throughout my academic journey, always believing in my capabilities and encouraging me to persevere.

A special mention must be made of my father, who constantly pushed me to strive for greatness and never settle for mediocrity.

I am profoundly thankful for my work colleagues, whose camaraderie and valuable insights have enriched my learning experience. A special mention goes to my loving wife, who has been a constant source of encouragement, inspiration, and understanding, and my children, whose presence has brought immense joy and motivation to my life.

I would also like to express my sincere appreciation to my supervisor, Dr. Adnan Maqsood, Director of Academics, NUST, who has played a crucial role in developing my understanding of aerospace systems. His expert guidance, constructive feedback, and unwavering support have been invaluable in helping me navigate the complexities of this field. Additionally, I am deeply grateful to my co-supervisor, Dr. Mian Ilyas and Dr. Shahzad Rasool for their unwavering support throughout this research. Their willingness to share knowledge and dedication to ensuring that the lab environment was conducive to learning have been genuinely inspiring.

Dedicated to my beloved wife, son, daughter, and Family, whose tremendous support and cooperation led me to this scholastic accomplishment

ABSTRACT

The last few decades has seen an unprecedented rise in global usage and deployment of autonomous aerial systems. Due to their affordability for common and versatile applications, ranging from aerial photography to highly sophisticated applications like surveillance and security, their popularity is growing exponentially. To increase efficiency and reduce exposure to hazardous scenarios, defense corporations worldwide are now focusing their development efforts on autonomous loitering munitions, which can be deployed at a tactical level and operated by an individual or a small crew. Armed Unmanned Aerial Systems have received more attention in recent years due to several advantages over manned aircraft such as long endurance and higher payload carrying capacity.

This thesis focuses on designing and developing loitering munition in the tactical / small UAS domain. The scope of work aims to conceive and create a proof of concept loitering munition, including the aerodynamic design cycle, selection and analysis of airfoil, wing sizing, drag polar analysis and mass budgeting. Performance Analysis pertaining to power-plant selection, propeller sizing, avionics selection, and appropriate battery selection is also conducted. The Prototype UAV has a tandem wing configuration with a frontal wingspan of 0.6 m and a rear wingspan of 0.45 m. The aircraft weighs 2.6 kg and has an L/D ratio of 15.7 owing to the high-lift requirements.

This research also encompasses the key aspect of prototyping and manufacturing. Using novel 3-d printing techniques, a prototype UAV is developed that establishes and validates key performance parameters, including mass budgeting, C.G. measurements, and aerodynamic performance. Various tests and activities are performed on the airframe, including mounting and integrating the complete avionics suite. Unpowered glide testing of UAV is performed using a UAV arresting Net. The prototype is equipped with IMU and Data Logging equipment to record various aerodynamic parameters during testing. Analysis of glide-test results indicates satisfactory lift performance as pitching angle of 15^{o} was achieved during the glide testing. The high-lift performance leads to improved payload carrying capacity and increased flight time in comparison with contemporary systems.

Table of Contents

Declaration ..... ***i***

Copyright Notice ..... ***ii***

Acknowledgments ..... ***iii***

ABSTRACT ***0***

1. Introduction ***6***

I. Origins and Evolution of Loitering Munition UAVs **6**

II. Motivation **7**

III. Research Objective and Problem Statement **8**

IV. Contribution **9**

2. Literature Review ***11***

I. Introduction **11**

II. Role and Niche of Loitering Munition UAVs **12**

III. Aerodynamic Design aspects: Lessons Learnt **14**

IV. Manufacturing Aspects: Lessons Learnt **16**

3. UAV Geometry, Sizing, and Aerodynamic Configuration ***18***

I. Geometry Definition and Initial UAV Sizing **18**

II. Aircraft Weight Estimation **18**

III. Airfoil Geometry **19**

a. NACA 24012 20
b. NACA 4412 21
c. NACA 25012 22
d. Conclusion and Final Selection 23

4. Aerodynamic Design and Performance Analysis ***25***

I. The Aircraft Drag Polar **25**

a. Preliminary Design Geometry 25
b. Drag Breakdown and Estimation 26

II. Power plant and Power Source Selection and Propeller Sizing **34**

a. Selection of Power plant 34
b. Selection of Propeller 37
c. Selection of Power Source 41

5. Avionics Architecture and Configuration ***43***

I. Top-level Architecture and Functionality **43**

II. Avionics Modules **46**

a. Autopilot 46

b. Actuators 48
c. Video and Data Link 50
d. Camera 50

6. Glide Testing: Methodology and Results *51*

I. Overview and Background **51**

II. Proposed Methodology **52**

III. Testing Results and Conclusion **55**

7. Conclusion *59*

I. Aerodynamic Design and Performance Analysis **59**

II. Propulsion System Selection and Analysis **59**

III. Avionics Architecture and Selection **60**

IV. Manufacturability Aspects and Prototyping **60**

V. Glide Testing Methodology and Validation **60**

8. Potential Improvements and Future Work *61*

I. Integration of Actuators **61**

II. Launcher **61**

III. Warhead performance **61**

IV. Avionics Suite **61**

Bibliography *62*

Abbreviation	Description
AR	Wing aspect ratio
Cd	Airfoil drag coefficient
CDo	Parasite drag coefficient
Cf	Friction coefficient for a flat plat
Cfe	Airfoil lift coefficient
Clmax	Maximum airfoil lift coefficient
CL	Wing lift coefficient
CLmax	Maximum wing lift coefficient

List of Abbreviations

D	Drag (N)
d	Propeller diameter (cm)
e	Oswald span efficiency factor
K	Induced drag coefficient
L	lift (N)
Pa	Power available from the motor/propeller for thrust
Re	Reynolds Number

List of Figures

Figure 1 Various UAVs under evaluation, Number, and Sources as Listed in Table 2 above....... 12
Figure 2 Switchblade ® Loitering Munition.. 14
Figure 3 Control Surfaces: Loitering Munition UAV (10) 16
Figure 4 Graphical rendering of Loitering Munition UAV.. 18
Figure 6 Coefficient of Lift VS Alpha- NACA 24012.. 20
Figure 7 Pitching Moment VS Alpha- NACA 24012.. 21
Figure 9 Coefficient of Lift VS Alpha- NACA 4412.. 21
Figure 10 C-Lift VS C-Drag- NACA 4412.. 22
Figure 12 Coefficient of Lift VS Alpha- NACA 25012.. 22
Figure 13 C-Lift VS C-Drag NACA 25012.. 23
Figure 14 Drag breakdown for a typical aircraft.. 27
Figure 15 Zero Lift Drag Variation with Speed.. 29
Figure 16 Wing Zero Lift Drag Coefficient.. 30

Figure 17 Rear Wing Zero Lift Drag Coefficient 31
Figure 18 Rear Wing Lift Induced Drag 32
Figure 19 Front Wing Lift Induced Drag 32
Figure 20 Drag Polar of the proposed design 34
Figure 21 3-blade 10 x 5 Propeller 39
Figure 22 Propeller Selection Chart (18) 40
Figure 23 System Elements and Configuration Items 43
Figure 24 Top-Level Avionics Architecture 45
Figure 25 Autopilot with Interface Details 47
Figure 26 JR Servo 318 Actuator 49
Figure 27 Cadxx Digital Camera Module 50
Figure 28 Centre of Gravity Study 53
Figure 29 Placement of Avionics Modules 54
Figure 30 UAV with Avionics Suite 54
Figure 31 Avionics Integrated in UAV using hatches 55
Figure 32 UAV approaching Net. 56
Figure 33 UAV arrested in Net. 56
Figure 34 UAV hanging from Net 57
Figure 35 Pitching Angle vs. Time 57

List of Tables

Table 1 Proposed specifications 8
Table 2 Performance Parameters of Various UAVs 11
Table 3 Comparison table: Loitering Munition, UCAV, and Cruise Missiles 14
Table 4 UAV Weight Distribution 19
Table 5 Aerodynamic Parameters 26
Table 6 Specifications of Power Plant 36
Table 7 Aircraft Performance Characteristics 49
Table 8 Video Link Performance Characteristics 50

1. Introduction

I. Origins and Evolution of Loitering Munition UAVs

A loitering munition or kamikaze drone refers to a broad class of UAVs capable of loitering over a target and homing in to destroy on impact. Since their inception, these UAVs can be classified as a hybrid between a cruise missile and a UAV. Sharing distinct characteristics of cruise missiles and UAVs, they are considered unique because of their prolonged hover and loiter times. The first drone of such kind was developed by IAI in the 1980s and was called Harpy [1]. Iran, Russia, the USA, and Israel developed early prototypes. Initial deployment remained limited to Suppression of Enemy Air Defence (SEAD) roles. The most notable deployment occurred in 1982 when Loitering Munition UAVs were seen destroying Syrian

Surface-to-air missile positions during the Syria-Israel conflict [2]. These UAVs were equipped with specialized sensors capable of detecting radars and air defense installations from a distance.

The turn of the millennia saw an unprecedented rise in the design and development of loitering munitions. Miniaturization and VLSI-based ICs significantly contributed to this upward trend. Introducing mini and tactical classes of UAVs was closely followed by loitering munition UAVs as global defense forces began placing orders for these [3]. US Army awarded multi-million dollars to AeroVironment for developing Switchblade ™ loitering munition UAV. In a similar vein, China, Turkey, India, Israel, and other countries began indigenous efforts to replicate.

Global warfare since the 2010s has seen significant usage of Loitering munition UAVs. The Armenia-Azerbeijan conflict of 2020 saw the fate of the battlefield tilt heavily in favor of the side which had Loitering Munition UAVs. The Russo-Ukraine war of 2022 has seen intensive use of Loitering munition UAVs by Ukrainian defense forces. Some defense analysts have called it the biggest obstacle in Russia's way.

II. Motivation

This research aims to conceive, conceptualize and develop a prototype of a loitering munition UAV with high agility, endurance, and efficient aerodynamic performance. The target specifications of the proposed loitering munition UAV are as follows:

Parameter	Specification
MTOW	2.6 kg
Range	2 km
Propulsion	Electric Motor + Propeller + LiPO Battery

Flight mode	Autonomous / PIC
Endurance	30-40 mins
Frontal Wingspan	680 mm
Rear Wingspan	600 mm

Table 1 Proposed specifications

This research has the potential to provide an indigenously developed loitering munition UAV to our Armed forces and security agencies. Pakistan faces a multi-faceted and multi-pronged hybrid war along its western borders which incurs regular losses to personnel and resource alike. An aerial platform like a loitering munition UAV can potentially turn the battlefield as it offers precision, lethality, and minimum probability of collateral damage.

III. Research Objective and Problem Statement

The research focuses on generating an optimal design for loitering munition UAVs that encapsulates mission requirements; user needs and proves economically viable. A study of contemporary systems and research material on the topic suggests that ease of deployment and cost remain at the forefront. Aerodynamic design efforts shall focus on fulfilling the objectives to cater to the criteria.

The following aspects of aerodynamic design are considered imperative and have been identified as primary research objectives for the successful design and development of Loitering munition UAV:

1. Geometry design
2. Aerofoil Selection
3. Drag Analysis
4. Lift Performance
5. Estimate Aerodynamic Performance Coefficients

6. Estimate W/S based on similar aircraft
7. Estimate Propulsion parameters
8. Estimate T/W and P/W
9. Calculate UAV performance parameters
10. Calculate the Centre of Gravity and Calculate Moments of Inertia

Furthermore, carrying out preliminary prototyping of Loitering munition UAV, selection of material, manufacturing scheme, and unpowered glide testing [4] is also one of the salient objectives. Avionics architecture will also be designed and implemented using COTS items and modules.

IV. Contribution

This research has the potential to significantly contribute towards the goal of indigenization of developing UAVs and aircraft in Pakistan. Rising import costs and the dire need for modern capabilities burden Pakistan's brittle economy.

This research contributes to advancing military technology and provides a basis for further research. The design and development of a cost-effective and user-friendly aerial platform such as a loitering munition UAV can prove an era-defining development in the field of aerospace.

Moreover, this research could have far-reaching implications on the broader spectrum not limited to loitering munition UAVs. Novel manufacturing techniques such as 3d printing can potentially revolutionize the aerospace sector. This research aims to synthesize a cost-effective yet exact manufacturing scheme that has the potential to find use in other aerospace and automotive products. This research will also cover the key aspect of prototyping and manufacturing. Using novel 3-d printing techniques, a prototype UAV shall be developed. This prototype UAV shall be utilized to establish and validate key performance parameters, including mass budgeting, C.G. measurements, and lift performance. Various tests and activities shall be performed on the airframe, including mounting and integrating the complete avionics suite. Unpowered glide testing of UAV shall be performed by using a UAV arresting Net. The prototype shall be equipped with IMU and Data Logging equipment to record various aerodynamic parameters during testing. The salient findings of this performance validation phase will aid in validating the design and proposed functionalities of the UAV.

2. Literature Review

I. Introduction

The domain of loitering munition UAVs has generated much interest in academia and industry since the late 1980s. Since Loitering munitions have been developed in all UAV categories, i.e., Mini, Tactical, and HALE, Aircraft designs similar or comparable to loitering munition UAVs were studied [5]. An exhaustive study of similar Mini, Tactical, and HALE classes of UAV systems was conducted. Data collection was focused on weight, geometry, size, velocity, and powerplant information. The table below presents this data, and the figure appended below shows a collage of the vehicles. Unfortunately, complete information was not available for all aircraft. Wing loadings would have been the preferred point of comparison rather than wing span and flight mass. Wing area data was unavailable for most of the comparable aircraft due to the unavailability of information.

Sr #	Designation	Classification	Wing Span (m)	Maximum Mass (kg)	Cruise Speed (m/s)	Source
1	**MLB 15 *cm* Trochoid**	MAV[1]	0.150		13.400	Design of MAVs (MLB Co.)
2	**University of Florida MAV**	MAV	0.152	0.055	11.170	Composite Materials for MAVs
3	**Black Widow**	MAV	0.152	0.050	12.630	defense-update.com
4	**MLB 20 *cm* Trochoid**	MAV	0.200		13.400	Design of MAVs (MLB Co.)
5	**Mosquito**	MAV	0.300	0.250	16.450	defense-update.com
6	**NRL MITE 2**	MAV	0.368	0.213	13.400	The NRL MITE Air Vehicle
7	**MLB Bat**	MPUAV[2]	0.600		13.400	Design of MAVs (MLB Co.)
8	**Wasp Block III**	MPUAV	0.723	6.530	13.410	USAF Fact Sheet
9	**BirdEye 100**	MPUAV	0.850	1.300		Israeli Aerospace Industries
10	**RQ-14B Dragon Eyes**	MPUAV	1.100	2.800	9.719	defense-update.com
11	**Desert Hawk**	MPUAV	1.320	3.200	16.662	defense-update.com
12	**RQ-11B Raven**	MPUAV	1.370	7.700	13.950	designation-systems.net
13	**BirdEye 500**	UAV[3]	2.000	5.000	18.000	defense-update.com
14	**Finder**	UAV	2.620	27.200	19.439	defense-update.com
15	**ScanEagle**	UAV	3.100	18.000	30.170	USAF Fact Sheet
16	**MQ-1 Predator**	UCAV[4]	14.800	1020.000	44.700	USAF Fact Sheet
17	**MP-9 Reaper**	UCAV	20.000	4750.000	102.800	USAF Fact Sheet
18	**RQ-4B Global Hawk**	HALE UAV[5]	39.800	14628.00	159.570	USAF Fact Sheet

[1] MAV: Micro Air Vehicle, [2] MPUAV: Man-Portable Air Vehicle, [3] UAV: Unmanned Air Vehicle, [4] UCAV: Unmanned Combat Air Vehicle, [5] HALE UAV: High-Altitude Long-Endurance UAV

Table 2 Performance Parameters of Various UAVs

Figure 1 Collage of various UAVs under evaluation, Number, and Sources as Listed in Table 2 above

II. Role and Niche of Loitering Munition UAVs

Historically, the role of Loitering munition UAVs has remained as a Suppression of Enemy Air Defense (SEAD) weapon. However, due to evolving battlefield requirements, the current role of Loitering Munition UAVs has expanded to include anti-personnel, anti-armor, anti-UAV, and targeting enemy supply lines.

Factors that include the complexity of deployment and reaction time make Loitering munition UAVs unique and distinctive. The ability to engage and disengage with targets at ground-level with real-time situation awareness has empowered commanders to make well-informed decisions which have resulted in minimizing collateral damages. Furthermore, cruise missiles and UCAV deployment usually involve multiple agencies and coordinate with multiple command tiers.

While some cruise missiles can loiter and have some terminal guidance control features, their primary function is to strike and not acquire target information. Cruise missiles are typically designed and optimized for long-range flight when selecting their aerodynamic configuration and propulsion system. Thus, it renders them unsuitable to loiter at slow fuel-efficient speeds, significantly reducing potential loiter capabilities [6].

The primary function of an armed UAV or UCAV is to carry out strike missions with prior target intelligence or a pre-defined mission area. Whereas most UAVs are designed with loitering capability, they are not optimized for a diving attack, often devoid of forward-facing cameras and sensors, and lack control response speed, which is redundant in typical UAV flights. UAVs are designed as multi-use platforms and utilize cutting-edge hardware and propulsion systems. These characteristics increase the unit cost of UAVs by manifolds, rendering them ineffective for one-time use [7].

Loitering munitions represent a paradigm shift in the realm of warfare, offering swift and adaptable deployment capabilities. By leveraging the synergy between unmanned aircraft and missile technology, these cutting-edge weapons can be dynamically deployed to the battlefield, catering to various combat missions and evolving battlefield conditions. Their multi-functionality encompasses reconnaissance, damage assessment, precision attacks, communication, and early warning capabilities [8]. With their extended endurance for prolonged aerial operations, loitering munitions hold a significant advantage in effectively engaging concealed adversaries positioned on elevated terrains, rooftops, and similar vantage points, substantially reducing casualties. Consequently, these munitions have garnered considerable attention in recent years, with several nations, such as the United States, Britain, and Israel, actively pursuing research and development in this domain. Their remarkable performance and practical utilization have underscored the integration of reconnaissance and attack capabilities within loitering munitions, marking a pivotal milestone in their deployment during combat operations. By enabling rapid and precise deployment of munitions over target areas, this innovative weaponry offers a compelling vision for future military engagements. Consequently, countries worldwide have intensified their research efforts on loitering munitions, focusing on emerging trends such as network cooperative engagement, composite guidance systems, human involvement in control loops, and developing cost-effective munitions [9].

Figure 2 Switchblade ® Loitering Munition

The following table compares the role and niche of Loitering munition UAVs with cruise missiles and Unmanned Combat Aerial vehicles:

Deployment Cost	Cruise Missile	Loitering Munition	Combat UAVs
Built-in Warhead	Yes	Yes	Yes
Expendable	Yes	Yes	No
Stealth features	Usually Yes	Usually No	Usually Yes
Loitering Capability	Usually No	Yes	Yes
Sensors for Target Detection	Yes	Yes	Yes
Command Control during Flight	No	Yes	Yes
Range	Up to 1500 km	Up to 1000 km	Up to 2500 km
Max Speed	High Sub-sonic	Sub-sonic	Sub-sonic
Endurance	< 2 hrs	10+ hours`	24+ hrs

Table 3 Comparison table: Loitering Munition, UCAV, and Cruise Missiles

III. Aerodynamic Design aspects: Lessons Learnt

Lessons learned from the study of contemporary systems and comparison with cruise missiles and Armed UAVs have been incorporated into the aerodynamic design cycle. First and foremost, the capability to loiter and hover over the target area while engaging the target in top-attack or nose-dive mode is a unique characteristic of loitering munition UAVs. Therefore, the aerodynamic design has to cater to this feature ab initio.

The high L/D ratio required for efficient performance and extended hovering maneuvers can be achieved by utilizing a tandem-wing configuration. Tandem-wing configuration entails two wings of similar wing area arranged in front of each other. This has some similarities with the canard configuration. The forward wing induces a downwash field on the rear wing, which subsequently causes higher induced drag on the aft wing. The rear wing can operate in the wake of the forward wing. However, aircraft designers need to be mindful of the distinct stall behavior of tandem wing configurations [10]. Rear wings are especially prone to stalling, especially if the two wing geometries are identical. The rear wing stall can cause unusually high pitch-up moments, which cannot be handled by autopilot in most cases. Thus, ensuring that the front wing always stalls before the rear wing is imperative. Our application requires a positive static margin design; consequently, the forward wing should have a higher lift load. One of the many methods to assist the front wing to stall before the rear wing is using alpha limiters. These can be both mechanical or electrical in nature. In this manner, control laws are modified to place an upper limit on the angle of attack. Inherently, tandem wing configurations are less vulnerable to stall, as when the higher wing-loading wing stalls, the other wing continues to generate lift. When the aircraft nose drops due to front-wing stall, it makes the airplane's angle (and its wings) less; the wing generates lift again once the aircraft's angle is good enough.

Tandem-wing aircraft have numerous advantages, which make them suitable for loitering munition UAVs. The center of gravity usually lies between the two wings. This makes the placement of avionics and other system elements much less cumbersome [11]. Moreover, the fuselage section's length can be varied per designer requirements. This flexibility in design is not available for typical aircraft configurations.

Another factor worth mentioning here is the weight allocation for avionics in the overall mass distribution of the aircraft. A study of contemporary systems has revealed that, unlike other aircraft categories, loitering munition UAVs have a much lower allocation for avionics in their overall mass distribution. The weight of avionics usually does not exceed 10% of MTOW, irrespective of weight class. This trend is seen in all research and development projects analyzed during this research. On second viewing, this aspect of loitering muntion UAV design seems intuitive. Conventional aircraft have to undertake multiple flights with rapid turn-around times.

Redundancy and Reliability in avionics add significant weight toll. Quality standards adherence is a tedious task that entails many aspects of qualification and testing.

Advancements in flight controllers and software algorithms imply that hybrid control surfaces (dual-purpose control surfaces) can now be adopted in UAV design, i.e., ruddervators, elevons, etc. This technique has been implemented in this proposed design by utilizing the concept of rudder-vators [12]. A control surface acts as a rudder for directional control and stability in one phase of flight and an elevator for additional lift generation in another phase of flight. This is enabled by more intelligent flight control computers which offer this dual-purpose control. The front wing control surfaces also act as ailerons for roll stability and control as and when required by the flight controller. This is in addition to their roll as lift-generating surfaces in the tandem wing configuration. This description is further elucidated in the figure below.

Figure 3 Control Surfaces: Loitering Munition UAV [13]

IV. Manufacturing Aspects: Lessons Learnt

3D printers have significantly impacted the Unmanned Aerial Vehicles (UAV) manufacturing process by offering several advantages and opportunities. This has disrupted the conventional methodology of manufacturing, which was heavily reliant on aerospace-grade alloys and composites. After market analysis, it became evident that the next generation of UAV manufacturers focuses on 3D printing.

3D printing allows for quick and cost-effective prototyping of UAV components. Design iterations can be easily implemented, tested, and refined, reducing the time and expense traditionally associated with prototyping. It also enables the creation of highly customized and complex designs that would be challenging or impossible to produce using traditional manufacturing methods. UAV components can be tailored to specific requirements, such as lightweight structures, intricate geometries, and integrated functionalities.

With 3D printing, UAV components can be manufactured using lightweight materials, such as advanced polymers and composite materials. This reduces the overall weight of the UAV, enhancing its performance, agility, and flight endurance. It facilitates on-demand manufacturing, allowing UAV components to be produced as needed. This eliminates the need for maintaining large inventories and enables quicker response times to changing requirements or urgent demands.

The financial aspect is a major driving factor in this shift to 3d printing. Although the initial investment in 3D printing equipment and materials may be significant, the overall cost of manufacturing UAV components can be reduced over time. This is particularly true for low-volume production, as the price per unit remains relatively constant regardless of the complexity of the design. It also provides an efficient means for producing replacement parts for UAVs, especially for older or discontinued models. This extends the lifespan of UAVs, reduces downtime, and minimizes reliance on external suppliers for spare parts.

Overall, 3D printers have revolutionized UAV manufacturing by offering greater design flexibility, faster prototyping, cost efficiencies, and the ability to produce complex, customized components. These advancements make it the most suitable method for manufacturing our proposed UAV design.

Conventional manufacturing methods involve development of tooling and molds which is a very time consuming process. This makes the conventional method unsuitable for rapid prototyping.

3. UAV Geometry, Sizing, and Aerodynamic Configuration

I. Geometry Definition and Initial UAV Sizing

A study of contemporary systems and literature review reveals no single best aircraft configuration. Aircraft design requirements can be translated in many ways. Table 2-1 elucidates proposed system specifications derived from user and operational requirements. Based on available data, system requirements, and user requirements, a tandem wing configuration is presented, as shown in the figure below.

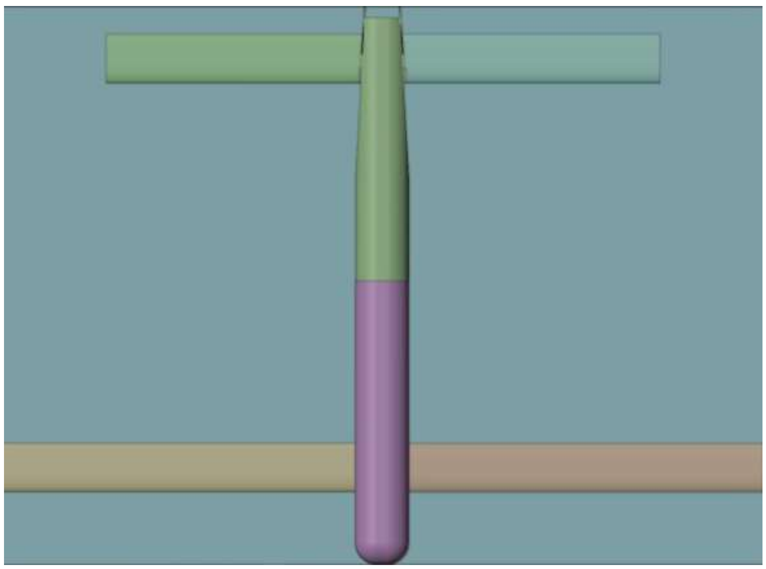

Figure 4 Top View of Loitering Munition UAV

II. Aircraft Weight Estimation

One of the primary tasks during the conceptual design phase of aircraft is the estimation of the MTOW of the UAV. Requirements dictate that UAV MTOW shall not exceed 2.6 kg. Gross MTOW can be ascertained using the following equation.

$$W_{TO=}\ W_{Struct} + W_{subs} + W_{prop} + W_{avionics} + W_{payload} + W_{energy} \quad \dots\dots\dots \quad (1)$$

Using knowledge of contemporary systems and literature review, the following weight allocations are assigned for UAVs. These allocations are tabulated below.

System Element	Weight (g)
Structure	300
Subsystem	50
Propulsion	600
Avionics	300
Payload	300
Energy	1000
MTOW	**2550**

Table 4 UAV Weight Distribution

Owing to the size and operational requirement of the UAV, it shall be manufactured using 3d printing technology. Lightweight materials such as polymers like bakelite/ABS will be used to manufacture the airframe. These materials weigh approximately 1 g/cm^2 [14].

To power the UAV, electric propulsion is proposed. The motor, propeller, and speed controller have been allocated 300 g of margin. The Avionics segment has been assigned 300 g of weight allocation. This will include a flight computer, data link, actuators, and cable harness. Energy weight allocation is 1000 g and shall consist of a high-density Lithium Polymer battery pack.

III. Airfoil Geometry

A natural starting point to begin UAV design is with airfoil design. This design aspect has a significant impact on whether the desired aerodynamic efficiency is achieved or not. Lift/Drag ratio, cruise speed, stall speed, and endurance are some performance characteristics being impacted by Airfoil selection. Multiple airfoils were analyzed based on theoretical and experimental data, a literature review, and a study of contemporary systems. NACA 24012, NACA 4412, and NACA 25012 were shortlisted based on superior lift performance characteristics. These airfoils are the popular choice among aircraft designers across the globe.

Defense companies like Aerovironment, IAI, and STM utilize this class of airfoils in their loitering munition UAVs.

Subsequently, the shortlisted profiles were analyzed further using XFLR aero design software. CM vs. Alpha and CL vs. Alpha performance was compared for all three airfoils. Graphical results for each evaluated airfoil are displayed below.

a. NACA 24012

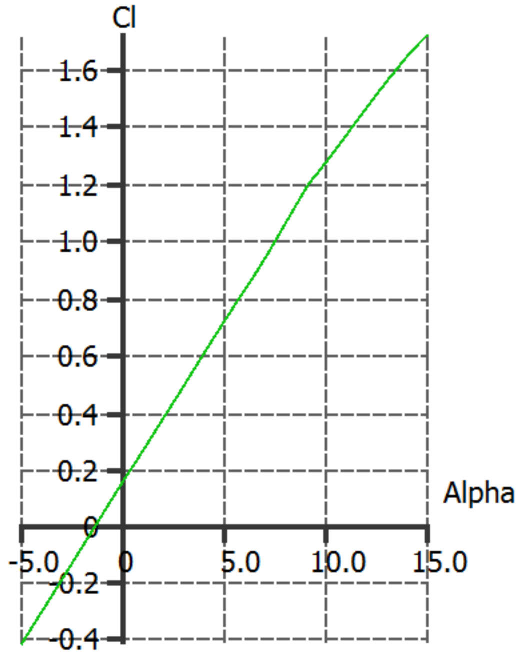

Figure 5 Coefficient of Lift VS Alpha- NACA 24012

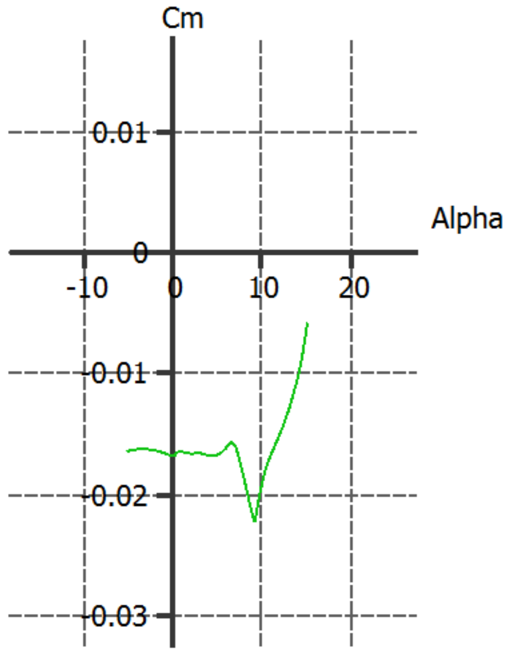

Figure 6 Pitching Moment VS Alpha- NACA 24012

b. NACA 4412

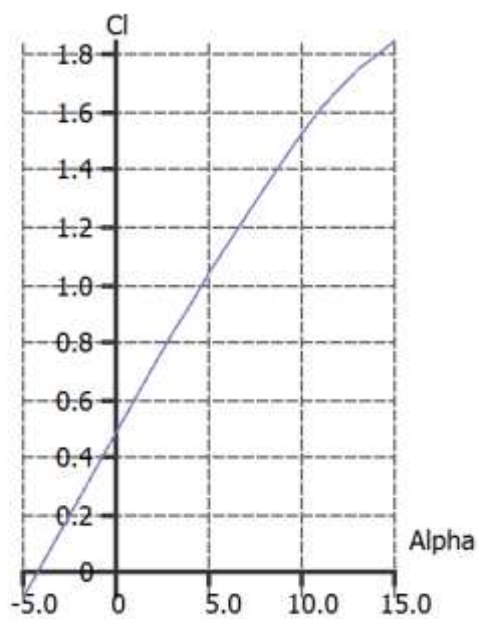

Figure 7 Coefficient of Lift VS Alpha- NACA 4412

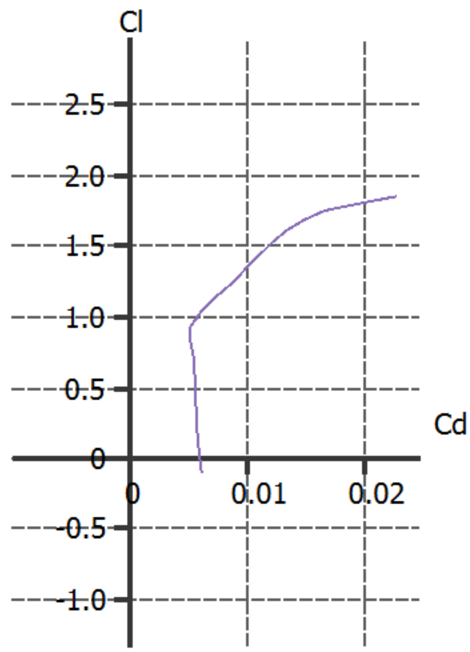

Figure 8 C-Lift VS C-Drag- NACA 4412

c. NACA 25012

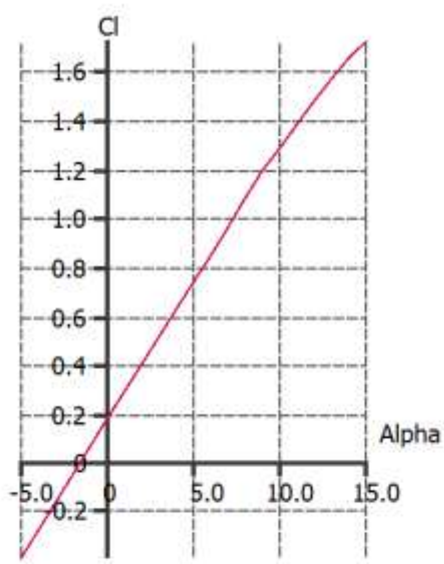

Figure 9 Coefficient of Lift VS Alpha- NACA 25012

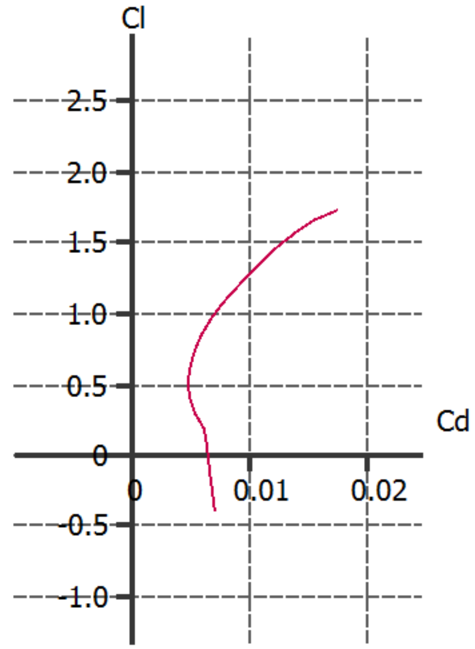

Figure 10 C-Lift VS C-Drag NACA 25012

d. Conclusion and Final Selection

All graphical and computational results were compared and analyzed. NACA 4412 was shortlisted as the airfoil for loitering munition UAV. Stall angle is an important factor for safety. NACA 4412 Airfoil has a higher stall angle, which ensures safety margins. The stall angle ranges from 16° to 18°. The design aim is to have a higher α greater than zero. Higher Cl max results in decreased stall speed, so higher Cl max is required for safe flight. The ideal coefficient of lift (Cli) is the Cl where Cd does not vary significantly with minor deviations of α. Cli corresponds to lower drag. Here it is necessary for low flight costs. The lift coefficient at zero angle of attack (Cl_0) is the Cl at α is zero. Cl_0 is better to design at High as it can produce a positive lift at a zero α. The nature of the Cl curve at and beyond the stall angle should be smooth. Airfoil has a gentle drop in the lift after stall, leading to a safer stall from which UAV can recover. [15]

The negative slope of Cm vs. Alpha is desired; it stabilizes flight even if α is disturbed. The tail component nullifies the value of Cm. The Cm should be close to zero as far as possible to have equilibrium in flight. Again NACA 4412 demonstrates the most optimum performance characteristics.

4. Aerodynamic Design and Performance Analysis

I. The Aircraft Drag Polar

a. Preliminary Design Geometry

Designing a new aircraft entails translating user requirements into a viable and feasible product. It is, therefore, imperative to elucidate the aircraft's intended purpose before proceeding with the conceptual design phase. Key aspects of catering before embarking on conceptual design are as follows:

- Defining the primary mission of the aircraft
- Defining Maximum Take-off weight and related parameters
- Defining cruise and maximum altitude
- Identifying stall, cruise, and maximum speeds
- Define the take-off landing scheme
- Defining whether mission requirements are being fulfilled

System specifications were generated after an exhaustive study and analysis of user requirements. These specifications were used as a baseline, and subsequently, salient aerodynamic parameters and configuration details were computed using AAA Software [16]. These parameters are tabulated below.

Specification	**Parameter**
Front Wing	
MTOW	2.6 kg
Wing Area	0.0247 m^2
Wing Span	0.61 m
AR	15.06
Taper Ratio	1
Mean Chord	0.004 m
t/c ratio	0.15
Wetted Area	0.0494 m^2

Airfoil	NACA 4412
Rear Wing	
Wing Area	0.0182 m^2
Wing Span	0.450596 m
AR	11.2
Taper Ratio	1
Mean Chord	0.004 m
t/c ratio	0.15
Wetted Area	0.0364 m^2
Airfoil	NACA 4412
Fuselage	
Length	0.46 m
Wetted Area	0.003 m^2
Max Cross section	0.0019m
Equivalent Diameter	0.05 m

Table 5 Aerodynamic Parameters

b. Drag Breakdown and Estimation

Aircraft have many constituent elements which can contribute to the overall drag depending on the chosen geometry: wing, fuselage, tail assembly, engine cowling, and canopy. The two main components of drag are parasitic and induced drag. It is pertinent to mention that the chosen concept aircraft operates outside the transonic or sonic flight regime, so wave drag is not considered in this analysis [17].

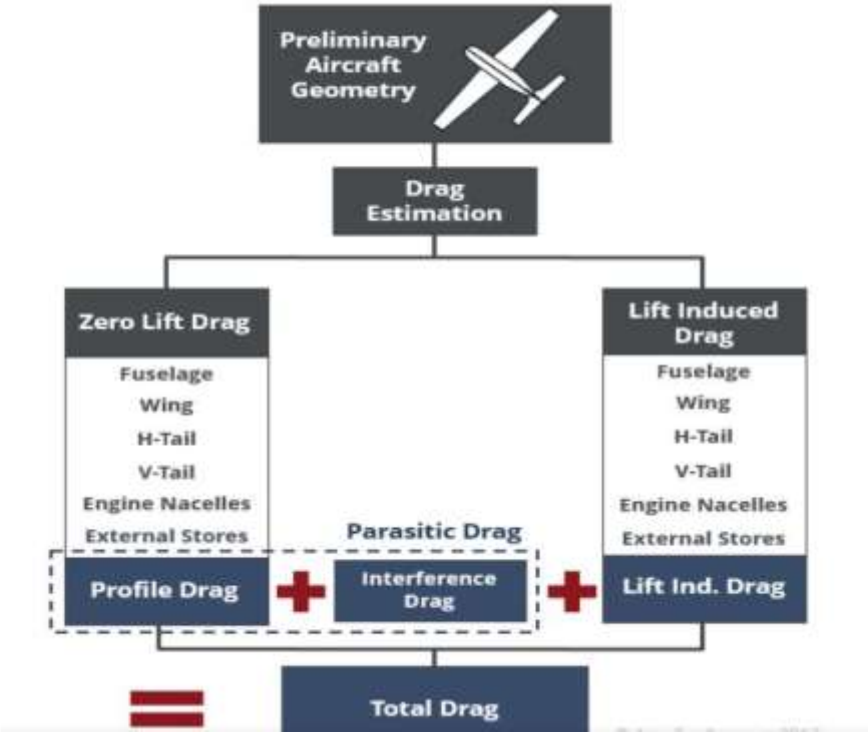

Figure 11 Drag breakdown for a typical aircraft

The total Drag of an aircraft can be computed as a sum of parasitic drag and lift-induced drag components, as shown by the equation below.

$$C_{D_{tot}} = C_{D_0} + C_{D_i} \qquad \ldots\ldots \quad (2)$$

$C_{D_{tot}}$: Total Drag

C_{D_0}: Zero-lift Drag

C_{D_i}: Lift-Induced Drag

Parasitic drag, also referred to as profile drag, is a type of aerodynamic drag that comes into play when an object is in motion through a fluid. It comprises a combination of form drag, stemming from changes in pressure due to the object's shape disrupting airflow, and skin friction drag, caused by the interaction between the fluid and the object's surface as they move. This phenomenon affects all objects moving through a fluid medium, regardless of their ability to generate lift.

Skin friction drag is a category of aerodynamic or hydrodynamic drag that manifests as a resisting force opposing the motion of an object in a fluid medium. This type of drag emerges due to the viscosity of fluids and transforms from a state of laminar drag to turbulent drag as the fluid flows across an object's surface. The transition from laminar to turbulent drag hinges on the specific fluid dynamics at the object's surface. The quantification of skin friction drag often involves the utilization of the Reynolds number, a dimensionless ratio that captures the equilibrium between inertial forces and viscous forces (Craig, 1998).

The cumulative drag experienced by an object can be deconstructed into two fundamental constituents: skin friction drag and pressure drag. Pressure drag encompasses diverse drag sources, encompassing even lift-induced drag, which can be perceived as an artificial abstraction. Lift-induced drag constitutes an aspect of the horizontal component of the aerodynamic reaction force.

As an alternative, the overall drag exerted on an object can be dissected into parasitic drag and lift-induced drag (Cook, 1999). Within this framework, parasitic drag encompasses all drag elements except for lift-induced drag. From this perspective, skin friction drag is categorized as a component of parasitic drag.

The zero-lift drag contribution of the fuselage is mainly influenced by both its wetted area and fineness ratio. This can be calculated using the formula provided below:

$$C_{D_{0(fus)}} = R_{wf} \cdot C_{f(fus)}\{1 + \frac{60}{(\frac{l_f}{d_f})^3} + 0.0025 \times (\frac{l_f}{d_f})\} \cdot \frac{S_{wetF}}{S_{ref}} \quad \ldots\ldots\ldots \quad (3)$$

Where:

$C_{f(fus)}$: Skin friction coefficient

l_f: Fuselage length

S_{wetF}: Fuselage wetted area

S_{ref}: Aircraft wing area

The skin friction coefficient can be obtained using the power curve fit of turbulent skin friction vs. the Reynolds Number graph from Roskam [18].

The graph below illustrates the fluctuation in zero-lift fuselage drag for the selected configuration. The drag coefficient has been calculated across the spectrum from the stall range to the maximum speed region

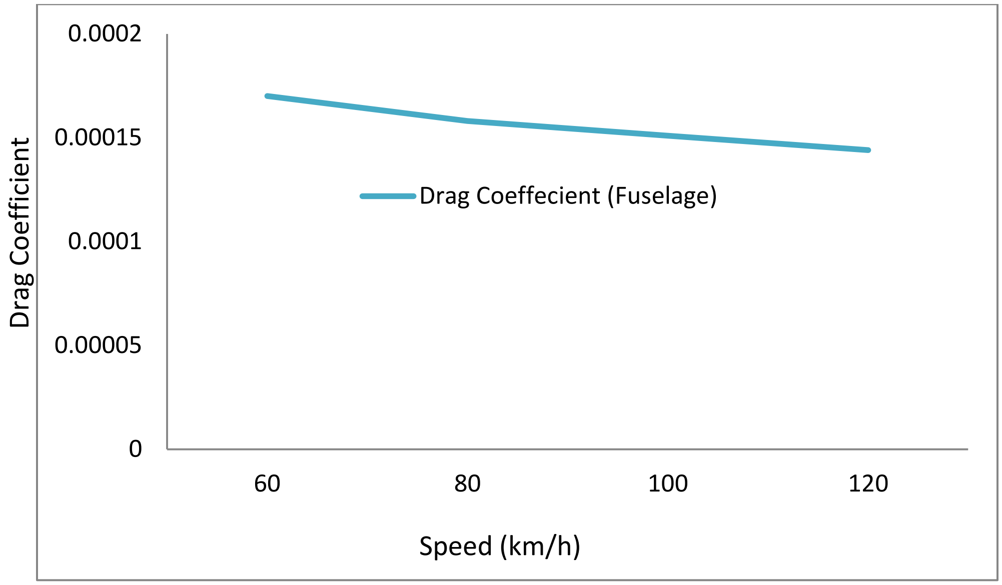

Figure 12 Zero Lift Drag Variation with Speed

We compute zero-lift drag contribution of the wing by using:

$$C_{D_{0(wing)}} = R_{wf} \cdot R_{LS} \cdot C_{f(wing)}\{1 + L^{*} \cdot (\frac{t}{c}) + 100 \cdot (\frac{t}{c})^{4}\}\frac{S_{wetW}}{S_{ref}} \quad \dots\dots\dots \quad (4)$$

Where:

R_{wf}: Wing Fuselage interference factor (Usually one is assumed for uniform surfaces)

R_{LS}: Lifting surface correction factor

$C_{f(wing)}$: Skin friction component of the wing

L^{*}: Airfoil thickness location parameter

t/c: Thickness to chord ratio

S_{wetW}: Wing-wetted area

S_{ref}: Aircraft reference area

The most influential factor in this context is the thickness/chord ratio. It is inferred that augmenting the wing's thickness leads to a more substantial drag contribution. Given the tandem wing setup, the calculation of zero-lift drag encompasses both the front and rear wings.

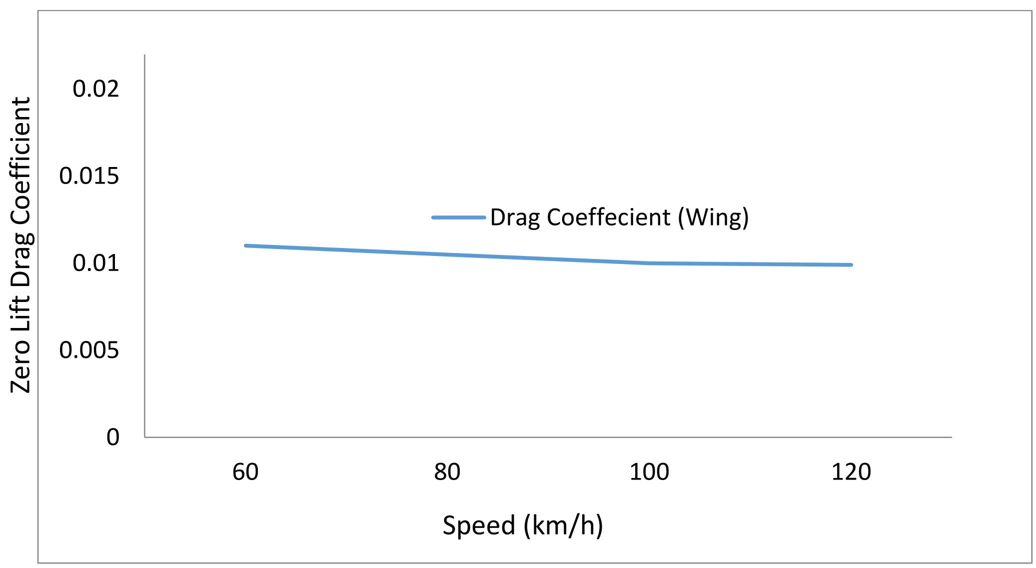

Figure 13 Wing Zero Lift Drag Coefficient

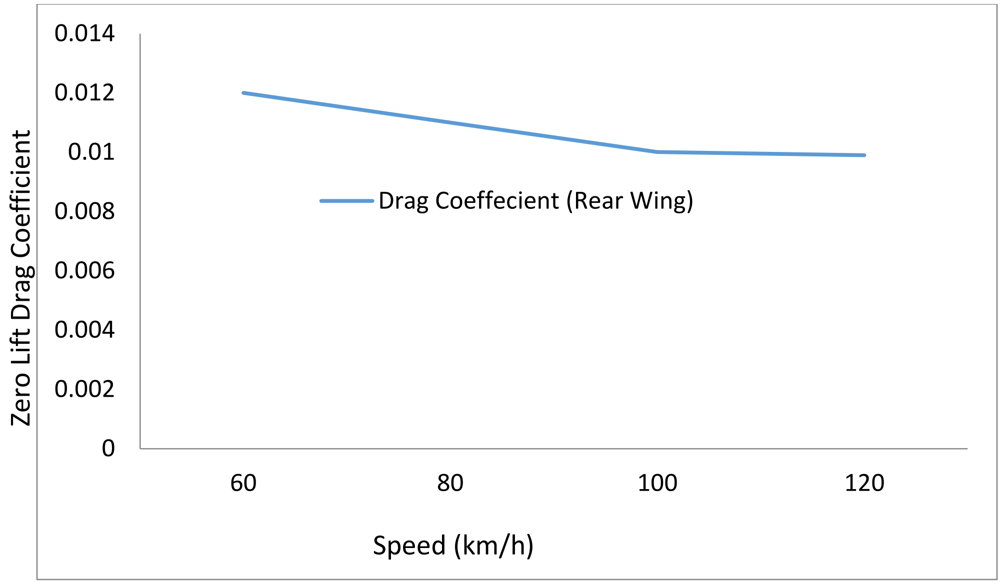

Figure 14 Rear Wing Zero Lift Drag Coefficient

Induced drag, also known as lift-induced drag, vortex drag, or drag due to lift, is an aerodynamic force that emerges whenever a moving object alters the direction of incoming airflow. This phenomenon is observed in airplanes, where wings or lifting bodies modify air motion to generate lift, as well as in cars equipped with airfoil wings that redirect air to create downforce.

When maintaining a constant level of lift, induced drag can be mitigated by increasing the aircraft's airspeed (Andersen, 2013). A counterintuitive outcome of this is that, up to the speed that yields minimum drag, airplanes require less power to achieve higher speeds. Another factor that reduces induced drag is an increased wingspan or the incorporation of wingtip devices.

The computation of Wing Lift Induced Drag can be accomplished through the utilization of the following formulae:

$$C_{di} = \frac{{C_{LW}}^2}{\pi \cdot AR \cdot e} \qquad \text{........ (5)}$$

Where:

C_{LW}: Lift produced by wing

AR: Aspect ratio of wing

The subsequent graphs illustrate how lift-induced drag behaves for the proposed design across the desired range of speeds.

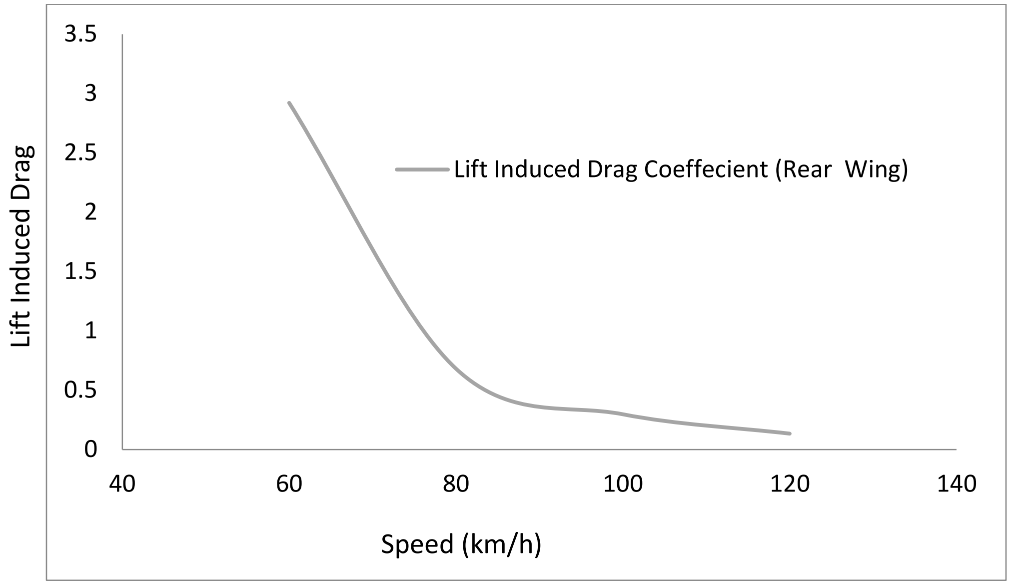

Figure 15 Rear Wing Lift Induced Drag

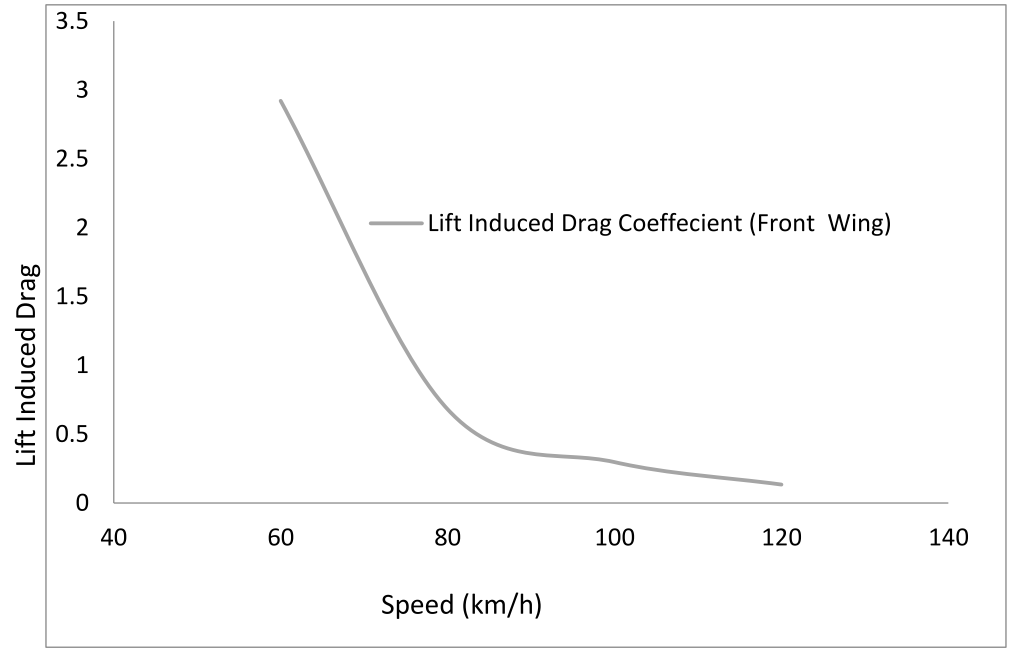

Figure 16 Front Wing Lift Induced Drag

The drag polar is a graphical representation illustrating the correlation between an aircraft's lift coefficient and its drag coefficient across a range of angles of attack (α), offering valuable insights into the aircraft's comprehensive performance within its flight envelope. The lift coefficient (CL) quantifies the lift generated by the aircraft's wings and depends on factors like angle of attack, airfoil shape, and aircraft configuration. Conversely, the drag coefficient (CD) characterizes the aerodynamic drag the aircraft experiences as it moves through the air. It's influenced by similar factors as the lift coefficient, along with airspeed, Reynolds number (Re), and Mach number (M). By plotting CL against CD for various angles of attack, the drag polar can be constructed, aiding in comprehending how alterations in angle of attack impact both lift and drag for the aircraft.

The point at which the lift-to-drag ratio attains its maximum value corresponds to the nadir of the drag plot, which is the point of minimum drag. The lift coefficient that is linked with this juncture forms the basis for the selection of the airfoil profile. It is advisable to opt for a profile that generates the least amount of drag at the desired lift coefficient.

Using the calculations and graphs compiled before, we obtain the Figure 17 Drag Polar of the proposed design for our proposed design.

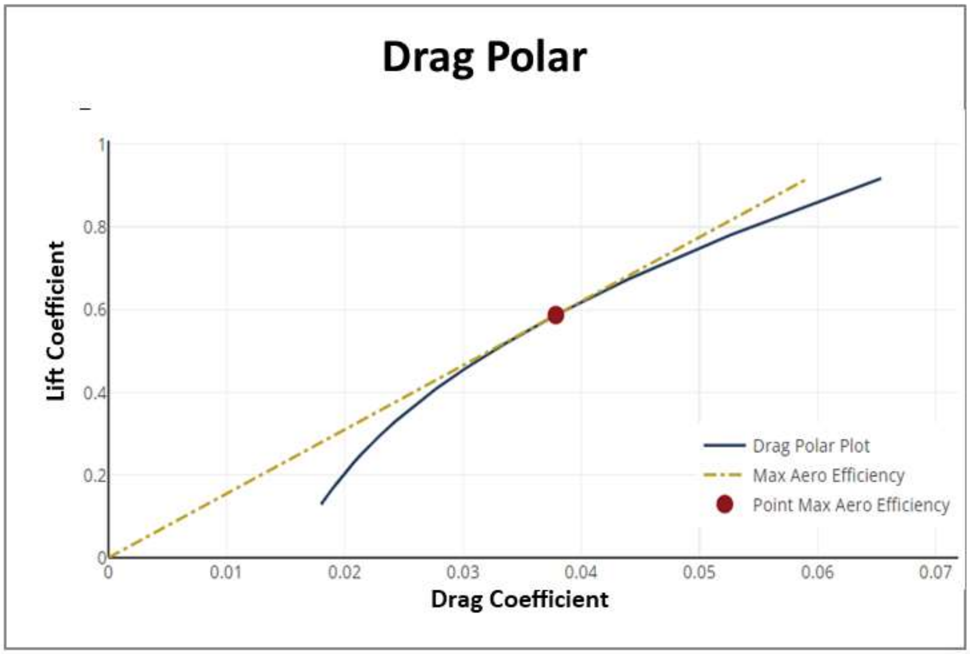

Figure 17 Drag Polar of the proposed design

II. Power plant and Power Source Selection and Propeller Sizing

a. Selection of Power plant

Unprecedented growth in aviation and aerospace technology domains has provided incremental improvements in each segment of aircraft design. Most notably, the surge in the development of tilt-rotor UAVs has paved the way for smarter and more efficient electric motors [19]. This rise in the use of electric motors has also been driven by sustainability and environmental factors related to the emission and burning of fuels.

Due to challenging weight, volume, and operational requirements, combustion or IC engines are deemed unsuitable for loitering munition UAVs. Electric motors are generally around 80-90 percent efficient, whereas IC engines provide 18-23 percent efficiency. Due to operational needs, the acoustic signature of IC engines being significantly higher than electric motors proves yet another impediment. Another stealth-related aspect of powerplant selection is the heat signature of the engine segment. IC engines have an inherently high heat signature which requires management and mitigation. Due to fewer moving parts and overall safety, electric motors are preferred in the Unmanned Aerial Vehicles domain.

The following options were analyzed for loitering munition:

- AC Motors
- Brushed DC Motors
- Brushless DC Motors

While AC motors are relatively inexpensive, they have two major drawbacks. Most notably, they are cumbersome to control and have sub-optimal power factor. While Brushed DC Motors have lower cost of construction, they remain vulnerable to heating issues and have lower operating speeds and lesser torque produced.

Brushless DC Motors provide the most suitable trade-off when performance characteristics are compared. Although they are more expensive than the other motors, they offer higher speed and torque at higher efficiency. Most critically, for our proposed design, they have smaller frame sizes and weigh significantly less than their counterparts [20]. Another key feature of electric motors is that they provide constant voltage against varying currents. This implies that the rotational rate remains constant irrespective of the load. The following characteristics of multiple motors were compared before the final selection:

- Maximum continuous horsepower
- Maximum torque vs. RPM Physical weight
- Physical dimensions
- Cooling techniques
- Required controller
- Gear reduction

After shortlisting the appropriate powerplant, the next step is determining the aircraft's required thrust. This thrust will provide a baseline to determine the power required.

We will use the information gathered to determine the aircraft's drag polar for the thrust requirement analysis. The following steps shall be executed to determine the thrust required:

1. Select a flight speed V.
2. Calculate CL from drag polar.
3. Calculate CD from the polar.
4. Calculate the efficiency E=CL/CD.
5. Calculate Thrust Required=W/E

Since the operational requirements define the maximum speed at 120 km/h, this value shall determine the maximum thrust required. Plugging in the values from the drag polar analysis and aircraft specifications, we get

W/E: 2550/14.67= 173.3 Watts

Based on thrust requirements, the Brushless DC Motor Long shaft KV950 power plant is selected for the loitering munition UAV. Salient features are tabulated below:

Parameter	Specification
Max Power	450 W
Weight	90 g
Peak Current	40 Amps
Dimensions	φ28.8 x 56 mm
Rated Voltage	2-4S LiPO

Table 6 Specifications of Power Plant

b. Selection of Propeller

The pivotal role of a propeller lies in transforming the rotational energy harnessed from the engine shaft into forward thrust, achieved by accelerating a mass of air roughly equal to the propeller's diameter. The resultant thrust is contingent upon three primary variables: the propeller's diameter, the count of its blades, and the inclination of these blades concerning the airflow.

A propeller propels a column of air having a diameter approximately matching its own dimensions. This generates a counter-directional thrust force that propels the aircraft ahead. The propeller's rotation imparts momentum to this air column, where momentum represents the product of the air's mass (determined by the propeller diameter) and its rearward velocity [21].

As a result, enlarging the propeller diameter diminishes the rearward velocity while sustaining the overall momentum imparted to the air. The propeller's energy is tantamount to the kinetic energy transmitted from the propeller to the air column. Given that total kinetic energy is determined by mass and the square of velocity, augmenting the mass of air (through increased propeller diameter) proves more energy-efficient than elevating the air velocity within a given energy state.

It is pertinent to mention that with escalating blade diameter, the moment of inertia of the blade increases exponentially. Moreover, a larger diameter propeller subjects the aircraft to notably augmented gyroscopic forces. These factors intensify the potential hazard of catastrophic blade failure, particularly during high rotational speeds.

The cumulative blade area of a propeller is determined by blade count, their width (chord), and the propeller diameter. Generally, larger engines producing higher power necessitate an augmented blade count to harness and effectively convert this power into propulsive thrust. [22].

By increasing the blade count we get the advantage of diminishing the shock and vibration experienced by the aircraft structure. In single-engine aircraft with a rear-mounted engine, each blade generates a pressure pulse during rotation that reverberates throughout the airframe. With a higher number of blades, the pressure pulses from individual blades become less impactful. Consequently, a propeller with three blades, for instance, inherently provides benefits in terms of smoother operation, reduced noise, and minimized vibration compared to an equivalent two-bladed setup.

Another critical consideration is the diameter of the propeller blade. A more powerful engine requires a larger blade area to extract maximum thrust at a given power setting. Blade area can be increased by adjusting the propeller diameter, increasing the chord (width) of the blades, or adding more blades. While a larger blade diameter is preferable, there are limitations. A significant increase in diameter leads to higher tip speeds, resulting in increased noise and drag as transonic speeds are approached [23]. Ground clearance must also be taken into account when enlarging the blade diameter. Moreover, increasing the blade chord may lead to decreased efficiency and reduced thrust due to increased blade interaction, known as the solidity ratio.

Therefore, increasing the number of blades becomes an optimal solution for efficiently extracting the desired thrust from an engine when a propeller with fewer blades cannot deliver the required thrust.

In the case of our conceptual aircraft, a choice between a two-bladed or three-bladed propeller should be made. While a three-bladed design may have slightly lower efficiency than an identical two-bladed design, improved vibration performance may make it the preferred option as the UAV mission requirements dictate it.

Propeller pitch broadly refers to the propeller's interaction with the air. Pitch refers to the angle at which the propeller blades are set relative to a flat plane. A fine-pitch propeller features a low blade angle, enabling easy rotation with a smaller air "bite" and shorter forward movement per revolution (low advance ratio). This configuration allows the engine to spin effortlessly and operate at high rotational speeds (RPM).

On contrary, a coarse-pitch propeller possesses a high blade angle, taking a larger bite out of the air with each revolution, resulting in greater forward movement. However, this coarse pitch setting limits the engine's operational speed and hinders its ability to achieve higher velocities.
We shall use a fine-pitch propeller for our chosen concept aircraft as our selected motor provides sufficient thrust throughout the flight envelope [24]. As the UAV will operate in a relatively higher speed regime, a coarsely pitched propeller is unsuitable for this application.

Manufacturers usually generate a data set that, among other variables, charts the propeller efficiency against a dimensionless parameter known as the advance ratio. This is done for each propeller configuration; i.e., this will be charted for a set of pitch angles and number of blades. These propeller charts can then be used to select a propeller based on three criteria; number of blades, pitch, and diameter.
The most effective way to size the propeller is to perform a sensitivity study around the three variables we have identified: the propeller's diameter, the blade pitch, and the number of blades. After studying the selection chart from NACA [25] recommended manufacturers [26], and the performance of our selected motor, a 10 x 5 3-blade propeller was shortlisted for our aircraft.

Figure 18 3-blade 10 x 5 Propeller

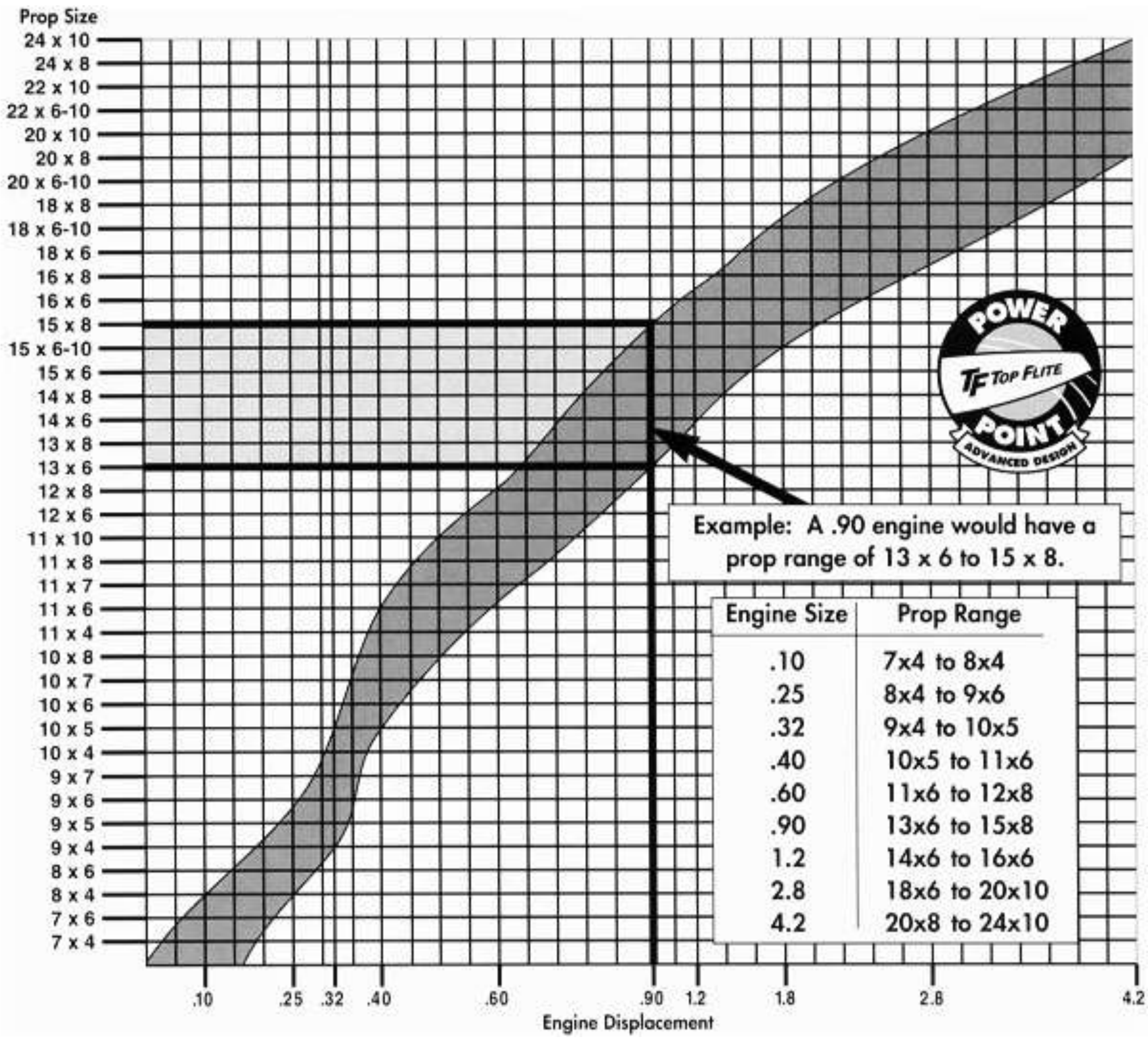

Figure 19 Propeller Selection Chart [27]

In the next stage, we need to quantify the effect of the larger blade pitch on the thrust produced at speeds around our flight envelope [28]. The efficiency is used directly in the calculation of the available thrust making use of the relationship between power, force, and velocity:

$$P_{shaft} = F_{thrust} \times V$$

$$P_{shaft} = P_{engine} \times \eta$$

$$F_{thrust} = \frac{P_{engine} \times \eta}{V}$$

$$F_{thrust}\ at \max speed = \frac{45.2 \times 450 \times 0.816}{20} = 98N \ \ldots\ldots\ldots \qquad (6)$$

c. Selection of Power Source

While selecting a battery for a UAV, it is important to consider key parameters such as voltage level, capacity (measured in milliamp hours), and discharge rate (the maximum current the battery can deliver). Other factors like activation time, charging time, lifespan, and cost also come into the equation during battery selection.

In the context of unmanned systems, different components, such as propulsion systems, processors, and sensors, often have varying voltage and load requirements. Moreover, different mission stages impose diverse power profiles, including takeoff, landing, hovering, and data gathering. As a result, the battery experiences fluctuating loads and must meet a wide range of demands.

In UAVs, the flight time is crucially dependent on battery life, and a complete battery drain during flight, known as a "dead stick" condition, can have disastrous consequences. A battery management system (BMS) is essential to mitigate this risk. The BMS continually monitors critical battery parameters, adapts to the varying power demands of the UAV's operations, and optimizes battery usage.

The battery management system monitors various battery parameters such as voltage, current, temperature, state of charge, and state of health. It may also derive additional information based on these measurements. In addition to regulating battery usage, the battery management system safeguards the battery during charging, protecting against overcurrent or over-voltage.

For our application, we first needed to specify some key parameters before making the final choice on battery selection. Since weight remains a critical consideration, the choice of battery type and capacity must be meticulously identified. Using the drone power calculations toolkit developed by Anvica et al. [29], we obtain the following parameters:

- Total system consumption= 5 A (Electric Motor + Avionics)
- Power required (0.5 hr flight) = 28 V x 5 Amps x 0.5 hrs= 70 W-hr

Rather than focusing on finding an optimal voltage, the user focuses instead with finding an ideal capacity and energy density. But it will also be more weight, just like if we maintained a 3S voltage but increased the capacity. This is a key observation because increased weight means increased power required to hover. Power does not increase linearly with the weight of the drone. Power is related to thrust by a factor of 3/2.

Keeping view of the above-mentioned considerations, the final choice of battery is an 8S (29.4 V) 3000 mAh battery pack. This provides sufficient capacity for the UAV to operate for more than 0.5 hrs in a variety of environments.

5. Avionics Architecture and Configuration

I. Top-level Architecture and Functionality

After a meticulous and detailed review of system requirements and preliminary aerodynamic design validation steps, selecting avionics components is the next step in the design cycle. The following sub-systems have been identified and further broken down into configuration items:

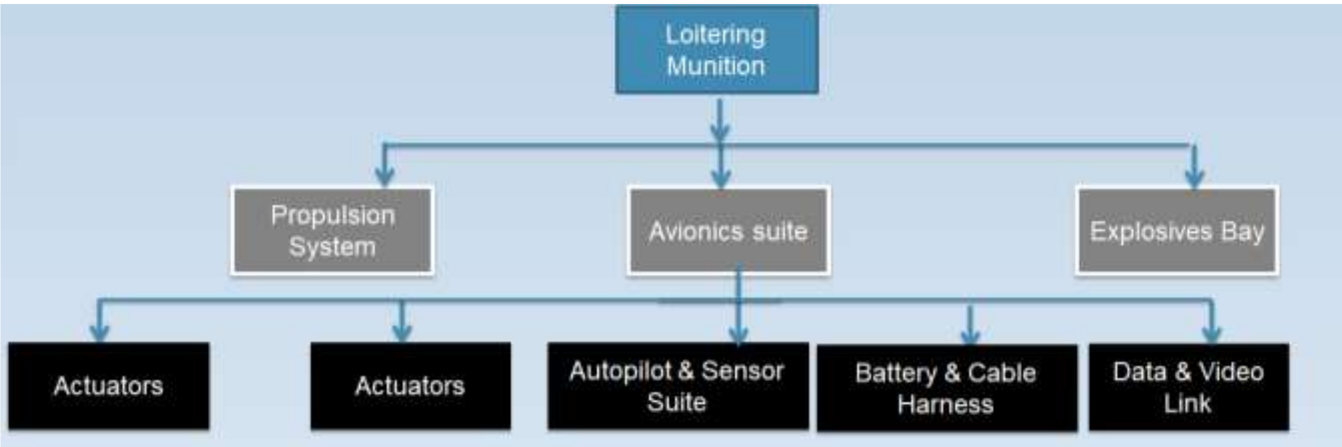

Figure 20 System Elements and Configuration Items

Based on user requirements and system specifications, selecting avionics components to achieve the desired functionality remains challenging. Due to stringent weight and volume constraints, all avionics packages shall cumulatively weigh no more than 300 grams and be packaged inside the fuselage. The available dimensions for packaging and housing of avionics are 100 x 30 x 160 (mm). Given the above, smartly packaged and lightweight avionics was sought. Moreover, after careful analysis, only flight and mission-critical avionics modules were selected for integration [30]. The following steps were undertaken to ensure compliance with stringent weight and volume considerations:

- Use of integrated Inertial and GPS Module- Autopilot shall have intrinsic sensors pack.
- Utilizing Day Camera with in-built Video and Data Link- Integrated solution.
- Minimizing Cable Harness weight by reducing nodes and connections.

- Selecting miniature and highly advanced Autopilot.
- Using Non MIL-STD Compliant Avionics without redundancy.

Interconnectivity and choice of interfaces were other aspects that needed detailed deliberation during the design phase. An optimization study was conducted to avoid level, power, and signal conversions. The Avionics bus was designed at a single voltage level to avoid EMI/EMC interference issues and the potential of unwanted ground loops. RS-485 Multi-drop serial interface actuators are proposed to reduce computational usage and cable harness. The system is equipped to handle both ground power and onboard battery power. 28 V and 5 V Actuator and Instrumentation buses were utilized, considering Aircraft design practices. The Top-level architecture diagram appended below explains the avionics architecture at length and specifies:

- Avionics Modules and their operating voltages
- Interfaces and Types
- Communication Protocol between modules
- Propulsion System electrical connectivity
- Propulsion System communication protocol
- Ground Power and Battery transition scheme
- Types and Gauges of Cable Harness
- Actuator Interfaces and Power connectivity
- Autopilot Internal Architecture, including multi-sensor pack
- Legend with all interface details with color codes
- Provision of Hot-plug as an Emergency Shut-down feature
- Data Logger and Ethernet Port for diagnostics
- Video and Data Link Interfaces and details

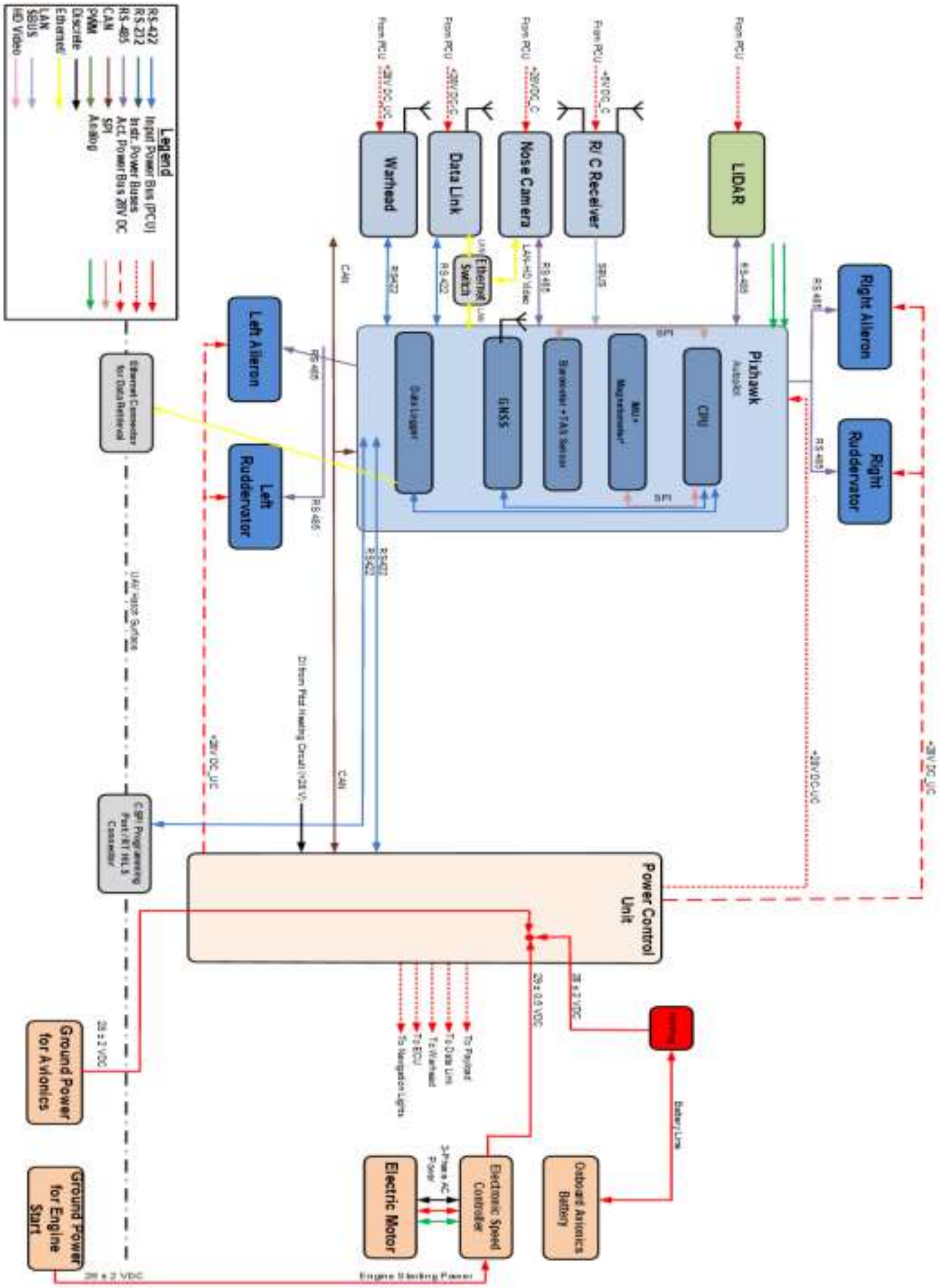

Figure 21 Top-Level Avionics Architecture

II. Avionics Modules

a. Autopilot

The primary hub of all flight-critical and mission-critical decision-making is the Autopilot. Therefore, selecting a suitable autopilot that fulfills all user and system requirements was of utmost importance. The following characteristics were identified for autopilot:

- Small form factor and minimum weight
- Integrated Sensor pack with GPS for Navigation and Control
- Ability to drive 4 x Actuator lines independently
- Able to control electric motor, including varying throttle and rpm as per flight requirements
- Compatible with commercially available battery packs
- Compatible with commercially available Video and Data Links
- Open-Source software suite for programming autopilot and peripherals

Considering the aforementioned criteria, Pixhawk ® Autopilot was shortlisted as the autopilot for Loitering Munition UAV.

Figure 22 Autopilot with Interface Details

Autopilot Features are summarized below:

- **Processor**
  - 32-bit ARM Cortex M4 core with FPU
  - 168 Mhz/256 KB RAM/2 MB Flash
  - 32-bit failsafe co-processor
- **Sensors**
  - MPU6000 as main accel and gyro
  - ST Micro 16-bit gyroscope
  - ST Micro 14-bit accelerometer/compass (magnetometer)
  - MEAS barometer
- **Power**
  - Ideal diode controller with automatic failover

- Servo rail high-power (7 V) and high-current ready
- All peripheral outputs are over-current protected, all inputs ESD protected

- **Interfaces**
  - 5x UART serial ports, 1 high-power capable, 2 with HW flow control
  - Spektrum DSM/DSM2/DSM-X Satellite input
  - Futaba S.BUS input (output not yet implemented)
  - PPM sum signal
  - RSSI (PWM or voltage) input
  - I2C, SPI, 2x CAN, USB
  - 3.3V and 6.6V ADC inputs
- **Dimensions**
  - Weight 38 g (1.3 oz)
  - Width 50 mm (2.0")
  - Height 15.5 mm (.6")
  - Length 81.5 mm (3.2")

b. Actuators

Like Autopilot, the selection of Actuators was also driven primarily by size and weight compliance. Mini and Tactical class of UAVs utilize mini-servos with high torque and rpm ratings. The control-surface sizing was based on the SAE Aero design standard for RC places [31]. The following table was used to determine the size of the control surfaces:

Control Surface	Aileron	Rudder	Elevator
Plan form surface ratio	SA/S = 0.03 − 0.12	SR /SV = 0.15−0.35	SA/ Sh = 0.15−0.40
Chord ratio	CA/C = 0.15 − 0.30	CR/CV = 0.15 − 0.40	CE/Ch = 0.20 − 0.40
Span ratio	bA b = 0.20 − 0.40	bR bV = 0.70-1	bE/ bh = 0.03 − 0.12

Results of control surface sizes were used to calculate hinge moments. AAA ® Software [32]. Hinge moments are a function of material density, control surface area, chord length, coefficient of hinge moment, and operating speed range. By using maximum speed and factor-of-safety of 1.5, we obtain:

Aileron hinge moment= 0.167 N-m

Elevator hinge moment= 0.364 N-m

Based on the aforementioned calculations, JR Servo 318 was shortlisted for Loitering Munition UAV. Rated torque and related performance parameters fulfill the criteria for selecting actuators for loitering munition UAVs.

Salient specifications of the actuator are tabulated below:

Parameter	Specification
Weight	6 grams
Dimensions	20×11.5×21mm
Max rated torque	Torque of 0.7kg-cm@4.8V
Max rated speed	Speed of 0.8sec/60°@4.8V

Table 7 Aircraft Performance Characteristics

Figure 23 JR Servo 318 Actuator

c. Video and Data Link

Another consideration for video/data link selection was low latency and high bandwidth. Ensuring these features in small form-factor and minimum weight toll posed a significant challenge. High-gain antennas provide much better coverage; however, weight and volume remain higher. Based on the above factors, Splash Drone 3 Video Transmitter ® was shortlisted as the video/data link. Specifications are tabulated below:

Parameter	Specification
Band	5.8 Ghz/600 mW
Weight / Dimensions	20 g / 31*23*9mm
Embedded Antenna gain	3 dB
Max range	5 km
Latency	4 ms

Table 8 Video Link Performance Characteristics

d. Camera

Camera feed quality and reliability is deemed critical mission requirement from the onset. Operators must rely on low-latency, high-quality imagery data for swift and well-informed decision-making. Based on this, Caddx Nebula Micro Digital/Analog Camera [33] was selected.

It provides ultra-low latency of 4 ms with 720p/60 fps HD Video. This camera is compatible with Ethernet and Serial interfaces.

Figure 24 Cadxx Digital Camera Module

6. Glide Testing: Methodology and Results

I. Overview and Background

Testing Unmanned Aerial Vehicles (UAVs) has historically posed significant challenges. The flight testing of UAVs requires additional measures beyond the standard performance evaluation [34]. The aeronautical industry acknowledges that the assessment of an air vehicle encompasses its flying qualities, flight performance, and avionics functionality. However, the ultimate determination of efficiency and cost-effectiveness rests on the comprehensive performance of the entire UAV system. Considerations of cost economics and safety drive this holistic solution.
Consequently, system reliability emerges as a crucial performance metric alongside flying qualities, flight performance, and avionics functionality. The system's reliability influences factors such as the loss rate of air vehicles, production quantities, maintenance demands, operating costs, and the overall viability of the solution. Additionally, the level of autonomy in the air vehicle has varying impacts on system reliability, contingent upon the maturity of the technology employed. The extent to which autonomous control can significantly enhance system reliability hinges on various factors that can only be ascertained with detailed knowledge of the specific system. Nonetheless, it is essential to emphasize that verifying reliability in a complex system necessitates structured testing [35]. This quandary, inherent to engineering, prevents the assessment of a system's economic feasibility in the absence of reliable data. Moreover, gathering such data entails substantial flight test risks, contributing to one of the major difficulties encountered in the flight testing of UAVs [36].

In addition to system reliability, there are other challenges pertaining to the applicability of manned aircraft flight test techniques to unmanned aircraft. As previously mentioned, the flight testing of UAVs can be categorized into the traditional domains of flying qualities, performance, and avionics evaluations. Regarding the evaluation of flying qualities, specific challenges arise due to the absence of control stick force feedback, lack of vibration and buffet response, and increased sensitivities in longitudinal, directional, and lateral control due to the compact size of the air vehicle. Furthermore, the absence of tactile acceleration cues experienced by pilots can pose a challenge when operating air vehicles with relatively low wing loading, high power loading, and low inertia.

However, recent advancements in electronics, rapid prototyping, and unmanned vehicle technologies have expanded their capabilities and reduced costs, increasing interest in academia and the industry. Based on this methodology, a rapid-prototyping approach for testing the proposed design was chosen.

II. Proposed Methodology

Flight test methodologies have been devised to evaluate compact electric-powered UAVs' performance effectively [37]. These techniques have proven successful in ascertaining crucial metrics such as the drag polar and performance parameters, including range, endurance, climb capability, and turn performance for UAVs. The methodologies encompass approximate measurements of aircraft dimensions and properties, meticulous calculations to characterize the motor-propeller combination's efficiency, and glide testing to determine the lift and drag coefficient across various velocities.

A prototype UAV will be launched and recovered in UAV Recovery Net. This UAV will have inertial sensors, GPS, and logging equipment to ascertain and validate flight performance. The primary focus will be on the pitch angle, roll stability, and yaw performance [38].

Prototype UAV was fitted with an avionics suite after ascertaining the C.G. and MoIs of the modules via ProE Software. After placement of all avionics modules in different locations and optimization study using the ProE tool, C.G. was determined to be 233 mm from the nose.

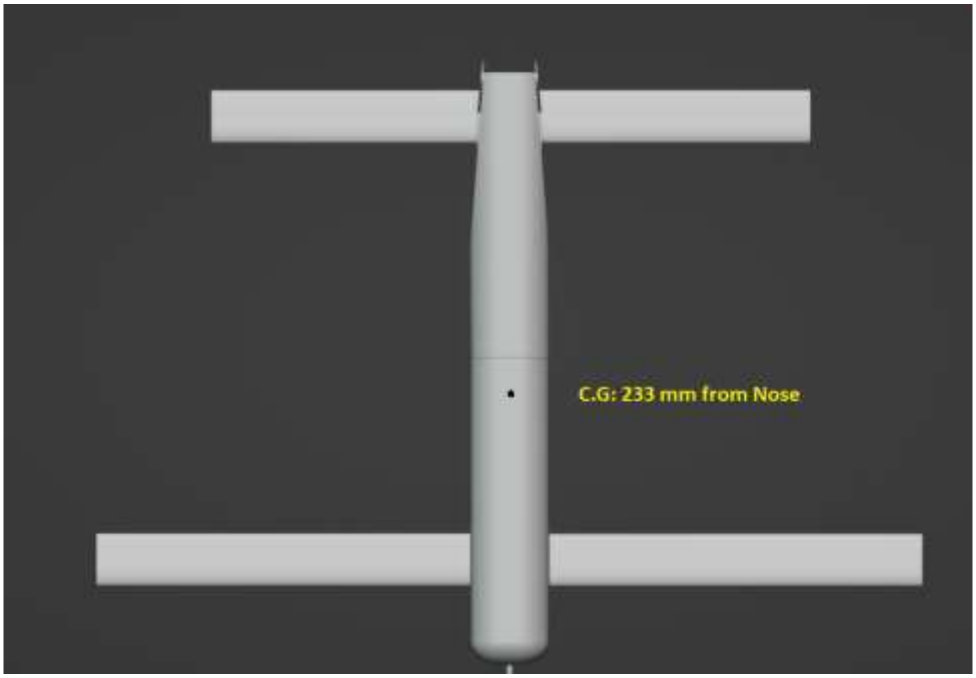

Figure 25 Centre of Gravity Study

The placement of avionics inside the UAV was adjusted to achieve the desired C.G. position. Special hatches were designed with avionics compartments to house all modules.

The testing equipment was installed in the UAV, and the arresting net was placed 3 m from the launch point [39].

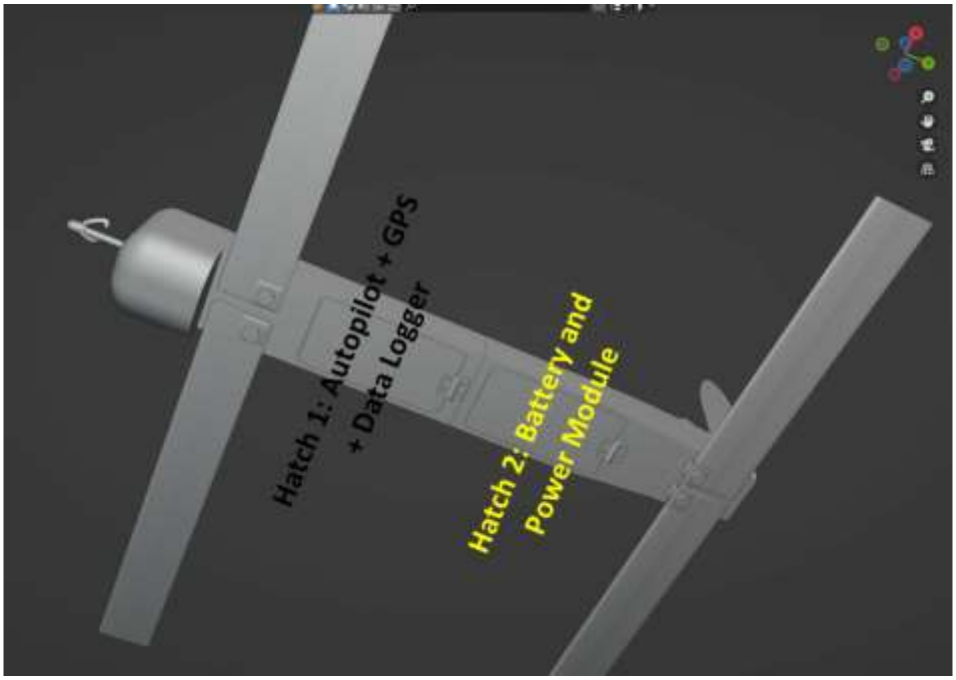

Figure 26 Placement of Avionics Modules

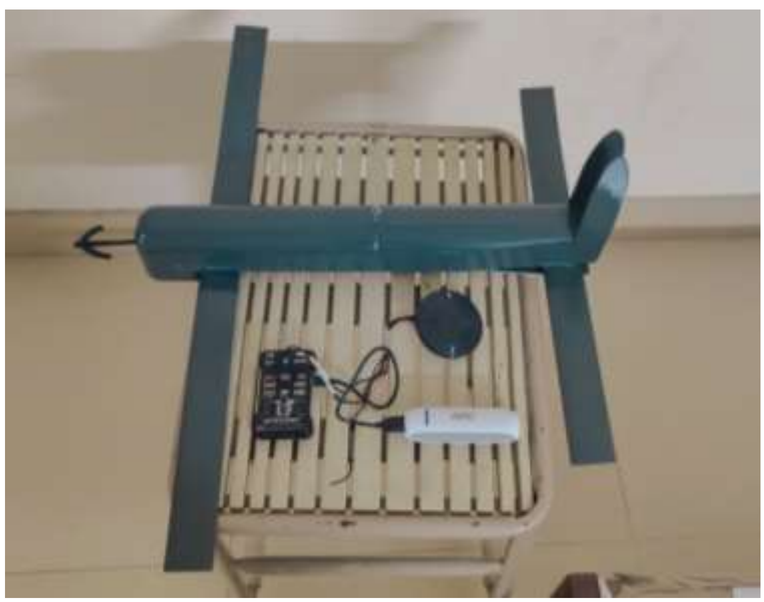

Figure 27 UAV with Avionics Suite

Figure 28 Avionics Integrated in UAV using hatches

III. Testing Results and Conclusion

The UAV was hand launched from a 3 m distance from the Net. The launch speed was 22 m/s, measured from the onboard GPS module and True Air Speed Sensor.

Figure 29 UAV approaching Net.

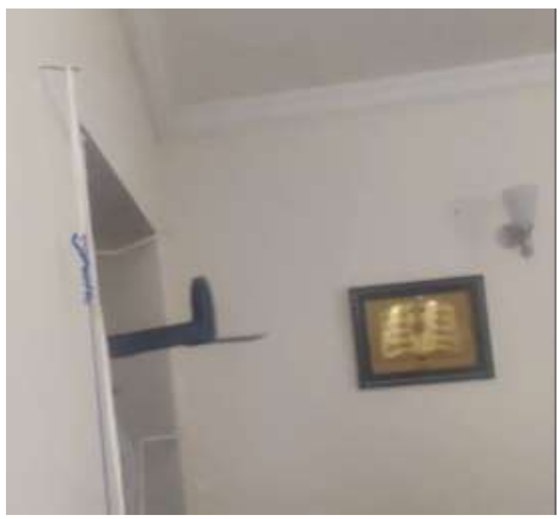

Figure 30 UAV arrested in Net.

Figure 31 UAV hanging from Net

The purpose of the experiment was to validate the lift performance of the aircraft. The most critical parameter to observe was the pitching angle of the aircraft during this hand-launched glide test.

The Figure 32 graph shows the pitching angle vs. time of the UAV.

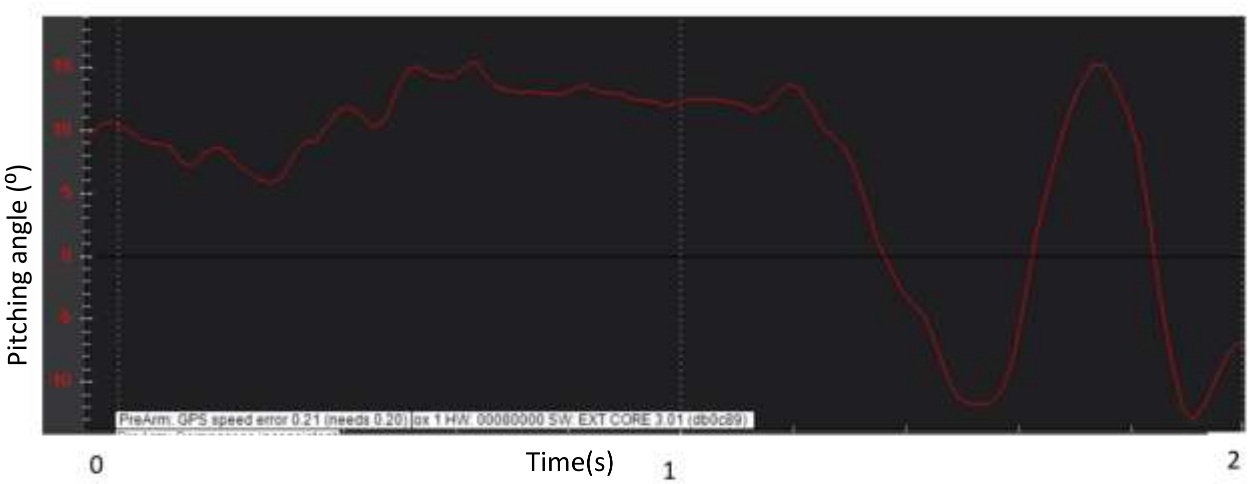

Figure 32 Pitching Angle vs. Time

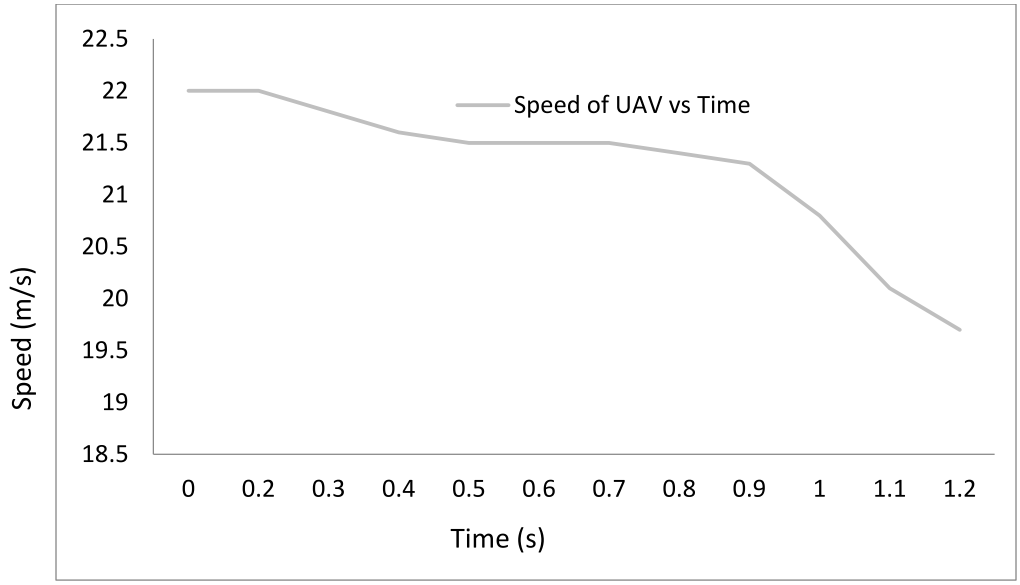

Figure 33 Speed of UAV vs. Time

The pitching angle of 15 degrees validates the lift performance of the aircraft. As predicted by the design, the lift performance of the aircraft was satisfactory. The choice of the airfoil, wing sizing, shape of the fuselage, and tandem wing configuration all contributed to this aero performance. Since the application of this UAV is deemed superior in lift characteristics, these test results reaffirm the design methodology. The figure above shows the speed profile vs. time of the UAV. It can be ascertained that the drag forces acting on the aircraft, as indicated by decreasing speed, were not significant. The airfoils generated sufficient lift to counter the drag forces.

7. Conclusion

From the onset, the research objectives of this thesis were proposing, analyzing, and validating a candidate design for a loitering munition UAV system. As elaborated in this section, these objectives were decomposed into various segments and compartments.

I. Aerodynamic Design and Performance Analysis

In order to establish a baseline aerodynamic design, the logical starting point was to select an appropriate airfoil. NACA series airfoils with high lift characteristics and excellent stall performance were shortlisted. By using XFLR5 ™ for characterization and performance comparison, NACA 4412 was considered the best choice among the candidates.

Wing sizing, fuselage shaping, and tail sizing were conducted using AAA ™ software, and abaseline geometry was established. Comprehensive drag-polar analysis was conducted since the primary focus was on designing a high-lift aircraft. Simulations and Analysis of various aerodynamic coefficients yielded encouraging results. A CAD Model was generated for the candidate design, a critical outcome of this phase. Another key aspect that was addressed in this phase was mass budgeting and allocation. This was imperative for the upcoming propulsion system and avionics design phases.

II. Propulsion System Selection and Analysis

An electric-motor-based propulsion scheme was devised after a literature review and study of contemporary systems. The thrust requirements were calculated using aerodynamic equations, and an appropriate electric motor was selected based on these results [40]. A key aspect of propulsion system design was propeller analysis. Based on system requirements, a 3-blade propeller was chosen for the candidate design. This choice was made considering the efficiency and improved vibration performance of 3-blade propellers. In order to meet endurance requirements, battery analysis was conducted, and an appropriate battery was proposed.

III. Avionics Architecture and Selection

An avionics suite was designed after a meticulous and detailed review of system requirements and considering the weight allocation. Functional-level baseline avionics architecture was developed. The challenging aspect was to achieve the mission and flight objectives while remaining in stringent weight margins. Autopilot, Data Link, Payload, and allied hardware were selected. This hardware was successfully integrated into the UAV and used in Glide Testing.

IV. Manufacturability Aspects and Prototyping

Utilizing the latest trends in manufacturing, the airframe was developed using 3-d printing technology. The airframe was decomposed into six different sections, and an assembly scheme was devised using ProE Toolset [41]. This resulted in a seamlessly integrated airframe with no assembly and related issues. The C.G. was determined after incorporating all weight-bearing members, including the propulsion system and avionics modules. The hatches were designed to ensure the C.G. is ensured throughout all phases of flight.

V. Glide Testing Methodology and Validation

After successful prototyping and integration of avionics, the next phase was glide testing. Scholars and scientists worldwide have proposed un-propelled glide testing to validate aerodynamic parameters.

8. Potential Improvements and Future Work

This thesis has achieved the desired objectives of designing and developing a prototype UAV. A comprehensive aero design was followed up by prototyping and integration of avionics. Despite this progress, many avenues and research opportunities emanate from this research. Some of these aspects are discussed in the coming section.

I. Integration of Actuators

An exciting area of research is integrating actuators in the UAV and conducting calibration and testing pertaining to their performance.

II. Launcher

UAV launchers are currently a very active area of research in academia and Industry alike. Designing and developing a suitable launcher for this UAV provides an excellent research opportunity.

III. Warhead performance

A critical feature of this UAV is the performance of the warhead. The lethality of a strike can be determined using simulation and modeling techniques in software like ANSYS® and MATLAB®.

IV. Avionics Suite

The evolving nature of technology means that avionics and aircraft equipment are undergoing a constant cycle of improvement. An optimization exercise can be carried out on the selected avionics suite to reduce the weight further and increase the flight time of the UAV.

Bibliography

[1] J. . J. 2. ". U. D. Federman, "Annual report DoD 2005". Department of Defense Publications 2005

[2] I. A. Report, "Modern Trends in UAV Design". Progress In Astronautics & Aeronautics, Vol. 180, No. 78, 2008.

[3] Z. Mahid And M. B. Khan, " Optimization Of Development of Loitering Munitions" AIAA Journal , Vol. 42, No. 10, , 2013.

[4] J. Neal, "FLIGHT TESTING SMALL, ELECTRIC POWERED UAVs". IEEE Aerospace And Electronic Systems Magazine, Vol. 15, No. 6, Pp. 15-17, 2000

[5] D. Raymer, Aircraft Design: A Conceptual Approach, Fourth Edition AIAA Education Press 2009.

[6] T. e. a. Takahashi, " "A multi-disciplinary survey of advanced subsonic tactical cruise missile configurations." 43rd AIAA Aerospace Sciences Meeting and Exhibit. 2005.".

[7] R. U. S. I. f. D. a. S. Studies, "UNMANNED COMBAT AIR VEHICLES: A Historical Perspective". International Symposium Of Ballistics, 2001.

[8] NAVAL POSTGRADUATE SCHOOL MONTEREY CA, "Design Requirements for Weaponizing Man-Portable UAS in Support of Counter-Sniper Operations". Journal Of Propulsion And Aeronautics, Vol. 86 2008

[9] Armenia Press Associate, "Armenian manufacturer boasts cutting-edge multifunctional combat UAVs and loitering munitions," 2022 .

[10] L. P, "Low-Reynolds Number Airfoils" In The International Conference On Applied Mechanics And Mechanical Engineering, 2014..

[11] M. T, "Aerodynamic Measurments at Low Reynolds Numbers for Fixed Wing Micro UAVs," 2018. *43rd AIAA Aerospace Sciences Meeting and Exhibit*, Reno, Nevada, January 2005, AIAA-2005-345.

[12] M. Selig, Airfoils at Low Speeds, In MATEC Web Of Conferences., 2017.

[13] Keith Andrews *Flight Testing of Fixed-Wing Aircraft*, American Institue of Aeronautics and Astronautics, 2003

[14] Bakelite, "bakelite Data sheet-OEM Issue 7" Dupont Technical Data Publications 2003.

[15] M. Sadraey, " Unmanned Aircraft Design: A Novel Approach". In International Conference On Aerospace Sciences And Aviation Technology., 2013.

[16] A. D. U. Manual. "3-d printing: A new era for prototyping" In International Conference On Fascinating Advancement In Mechanical Engineering , 2012

[17] K. Nickel, " Tailless Aircraft in theory and Practice, American Institute of Aeronautics and Astronautics," *AIAA Journal,* 1997.

[18] J Roskam, Prelimnary Aircraft Design DARCorporation Publications 2015.

[19] S. Morris, "Design and Flight Test Results for Micro-Sized Fixed-Wing", 1st AIAA International Futuristic Technologies Conference, 2017.

[20] Grasmeyer, "Development of the Black Widow UAV," in *39th AIAA Aerospace Sciences Meeting & Exhibit.*, 2001.

[21] T. J., "“Micro Aerial Vehicle Development," Defence Science Journal , Vol. 70, No. 3, 2020.

[22] T. J, "Design of a Tube-Launched UAV," Proceedings Of CERME, Vol. 8, Pp. 970-979, 2013.

[23] J. Deivey, " Subsonic Aircraft design. Applied Computational Aerodynamics, Vol. 125," 2000.

[24] G. Robertson, " Control of a Swept Wing tailless Aircraft," AIAA Journal., Vol. 78, No. 6, Pp. 616-619, 2010.

[25] N. A. S. Datasheet, "https://history.nasa.gov/naca/". NASA Publications Press 1968

[26] T. F. P. C. OEM, "http://www.top-flite.com/accys/topq5000a.html". Technical Data Sheet Bakelite ™ 2008

[27] R. P. Forum, "https://www.rc-airplane-world.com/propeller-size.html," [Online].

[28] S. Murray, "Ground and flight evaluation of a small-scale inflatable-winged aircraft," 8th AIAA Applied Aerodynamics Conference. 2010.

[29] U. P. Characterization, "https://www.translatorscafe.com/unit-converter/en-US/calculator/multicopter-lipo-battery/". Online. 2013

[30] G. Budd, "Operation and Research Aspects of Radio Controlled Flight Test Program," 5th AIAA Aerospace Sciences Meeting. 1997.

[31] Márquez, R. A., Martínez, M. A., & Martínez, M. J. (2021). Control surface design for radio-controlled aircraft. Case: SAE Aero Design Micro-class prototype. *Revista Facultad De Ingeniería Universidad De Antioquia*, (104), 71–82.

[32] D. Software, *https://www.darcorp.com/advanced-aircraft-analysis-software/.* DARCorporation Freeware Manual 2007

[33] Cadxx, "https://caddxfpv.com/collections/analog-camera-1/products/caddx-nebula-micro-digital-analog-camera?variant=39806805770339". Cadex Online Catalogue 2023.

[34] W. W, "The Challenges of Flight-Testing Unmanned Air Vehicles" The Aeronautical Journal vol 197.2018.

[35] Foster T. and Bowman J., “Dynamic Stability and Handling Qualities of Small Unmanned-Aerial Vehicles,” *43rd AIAA Aerospace Sciences Meeting and Exhibit*, Reno, Nevada, January 2005, AIAA-2006-1023.

[36] Higashino S. and Ly U., “Development of a UAV Flight-Test Vehicle at the University of Washington,” *2nd AIAA “Unmanned Unlimited” Systems, Technologies, and Operations, Workshop and Exhibit*, September 2003, AIAA 2003–6583.

[37] S. Higashino, "Development of a UAV Flight-Test Vehicle at the University of Washington,," *2nd AIAA “Unmanned Unlimited“ Systems, Technologies, and,* 2002.

[38] J Brinker J. and Wise K., “Flight Testing of Reconfigurable Control Law on the X-36 Tailless Aircraft,” *AIAA Journal of Guidance, Control and Dynamics*, Vol. 24, No. 5, Sep.-Oct. 2001, pp. 903–909.

[39] Ostler, Jon & Bowman, W.. (2005). Flight Testing of Small, Electric Powered Unmanned Aerial Vehicles. 10.2514/6.2005-7654.

[40] Murray J. E., Pahle J. W., Thornton S. V., Vogus S., Mello T. F. J. D., and Norton B., "Ground and Flight Evaluation of a Small-scale Inflatable-winged Aircraft," *40th AIAA Aerospace Sciences Meeting and Exhibit*, Reno, Nevada, January 2002, AIAA-2002-0820.

[41] S. Jenkins, "Composite Materials for Micro Air Vehicles.," in *Proceedings of the SAMPE Annual Conference*, 2011.

[42] Seanor A., *Flight Testing of a Remotely Piloted Vehicle for Aircraft Parameter Estimation Purposes*, Ph.D. thesis, West Virginia University, Virginia, 2002.

[43] Budd G., "Operation and Research Aspects of Radio Controlled Flight Test Program," *Tech. rep., 1993, NASA Technical Memorandum*, 104266.

[44]] Hiller B., "Estimation of Drag Characteristics of a Fixed Wing Unmanned Aerial Vehicle," *AIAA's 1st Technical Conference and Workshop on Unmanned Aerospace Vehicles*, Portsmouth, Virginia, May 2002, AIAA-2002-3495.

[45] J. Anderson, Introduction to Flight, McGraw Hill Publications 2003.